Vegetation and fire variability in the central Cerrados (Brazil) during the Pleistocene-Holocene transition was influenced by oscillations in the SASM boundary belt

Quaternary Science Reviews Volume 232, 15 March 2020, 106209

https://doi.org/10.1016/j.quascirev.2020.106209

Raquel Franco Cassino [(1)*]; Marie-Pierre Ledru [(2)]; Rudney de Almeida Santos [(2,3)]; Charly Favier [(2)]

[(1)]Departamento de Geologia, Universidade Federal de Ouro Preto, Brazil; [(2)]Institut des Sciences de l'Évolution de Montpellier, Université de Montpellier CNRS IRD EPHE, France; [(3)]Universidade de São Paulo, Brazil.

*corresponding author (address: Departamento de Geologia, Universidade Federal de Ouro Preto/Campus Morro do Cruzeiro, Bauxita, 35400-000, Ouro Preto, Brazil. E-mail address: raquelcassino@ufop.edu.br)

Abstract

This study investigates historical fire regimes and arboreal cover variability in the Brazilian Cerrados, a large Neotropical savanna ecosystem, during the Pleistocene-Holocene transition and early Holocene, and then tests whether the observed variation is linked to South American Summer Monsoon (SASM) variability. We present high-resolution pollen, XRF and charcoal records from lake Lagoa Feia, located in central Cerrados, and assess how they compare with other pollen records from the surrounding region to investigate regional trends of vegetation and fire regime variability. Our results show that the Pleistocene-Holocene transition was marked by a wet episode, which included moist forest expansion and rising lake levels, that correlates well with increased monsoon activity in a large area of central South America during the same period. This wet episode chronologically coincides with the Younger Dryas cold episode in the northern hemisphere. Our data revealed moisture declines in central Cerrados after 11.2 kyr BP, along with centennial-scale fluctuations from dry to wet conditions throughout the early Holocene period until around 6 kyr BP. These dry/wet oscillations are associated with weakened SASM activity and repeated shifts of its belt position during this time range. Fire activity increased in central Cerrados just after the onset of drier conditions during the early Holocene, and likely contributed to decreased arboreal cover at that time. A trend of increasing moisture in the region was observed after 6 kyr BP. Our study reveals how centennial and millennial-scale changes in monsoon activity influenced arboreal cover, diversity and fire regimes in the central Cerrados.

Keywords: Brazil; Termination 1; fire; pollen; tropical savanna; Paleoclimatology

1. Introduction

The Brazilian Cerrados is the second largest biome of the Neotropics, covering about 2 million km² of tropical South America (Fig. 1A). The vegetation of the Cerrados is classified as a moist savanna and comprises open savannas, savanna woodlands, grasslands and shrubby grasslands, dry forests and riverine forests (Furley, 1999). The wide range of latitudes - 2° to 24°S – across which this biome stretches entails significant climatic variability across the region, but the occurrence of a strong dry season during

austral winter (usually spanning four to six months) is common to the whole biome (Oliveira-Filho & Ratter, 2002; Fig. 1B). Rainfall is concentrated in the austral summer months, and is influenced by South American Summer Monsoon (SASM) activity (Silva & Kousky, 2012). The distribution of the Cerrados also coincides with the highly weathered, nutrient-poor soils found in the plateaus of central Brazil (Motta *et al*., 2002, Oliveira-Filho & Ratter, 2002). In addition to rainfall seasonality and dystrophic soils, fire is an important factor in the maintenance of the physiognomic and floristic diversity of the Cerrados (Hoffman & Moreira, 2002). Most of the flora found in the Cerrados is adapted to, or dependent on, fire; as such, the origin and diversification of these plant lineages are, to a great extent, related to fire-resistant adaptations (Simon *et al*., 2009).

Past changes in the structure and composition of vegetation cover in the Cerrados can be considered a result of variations in rainfall amount and seasonality and/or of changes in the fire regime. SASM activity is known to have varied at the millennial scale as a response to variations in Southern Hemisphere (SH) insolation, which occur at orbital cycles of *ca*. 20 kyr (Kutzbach *et al*., 2008). SASM activity and SH insolation are positively correlated in that monsoon circulation and precipitation in the SH is enhanced when SH insolation is at a maximum (Cruz *et al*., 2005; Kutzbach *et al*., 2008). Increased SASM convective activity is caused by modifications in the interhemispheric temperature gradient – which is significantly controlled by summer insolation – that results in southward shifts of the Intertropical Convergence Zone (ITCZ) and South Atlantic Convergence Zone (SACZ) (Cheng *et al*., 2013; Schneider *et al*., 2014), main features of the SASM system. Other mechanisms besides insolation variability have also been documented to affect the interhemispheric temperature gradient, as well as influence the ITCZ/SACZ systems; for example, Heinrich events of massive ice melting in the North Atlantic have also been related to SASM variability (Kutzbach *et al*., 2008; Strikis *et al*., 2015; Rojas *et al*., 2016).

Late Quaternary speleothem δO^{18} records from southern Brazil (Botuverá cave (Cruz *et al*., 2005; Wang *et al*., 2007)), central-western Brazil (Jaraguá cave (Novello *et al*., 2017), and central-eastern Brazil (Lapa Grande and Lapa Sem Fim caves (Strikis *et al*., 2015; 2018) have been used to track changes in SASM position and activity over the last glacial cycle because they show significant co-variance with SH summer insolation and/or cold episodes in the North Atlantic. These speleothem records show differences that are

related to their latitude (from northern to southern Brazil) and, as such, can be used to infer shifts in SASM belt activity and amplitude (Maslin *et al*., 2011).

Speleothem records show a succession of wet/dry events during the late Pleistocene and Holocene. Dry events with reduced rainfall over central and southern SASM regions were observed during warmer NH conditions (14.7 to 12.9 kyr BP) (Wang *et al*., 2007; Novello *et al*., 2017), while the return of colder NH conditions during the Younger Dryas event (12.9 to 11.7 kyr BP) resulted in increased moisture across southern, central-eastern and western South America (Wang *et al*., 2007; Novello *et al*., 2017; Stríkis *et al*., 2018). During the early Holocene, the onset of relatively drier conditions in the SASM region was again correlated with warmer NH conditions (Novello *et al*., 2017; Cruz *et al*., 2005). From the middle Holocene onwards, a general trend towards wetter conditions was observed in southern Brazil (Cruz *et al*., 2005). Conversely, in the eastern Amazon, the spelothem record from the Paraíso cave (Wang *et al*., 2017) shows peak of high humidity around 6,000 yr BP and then a tendency of decrease in rainfall amount until the present. In central-eastern Brazil, the Holocene was punctuated by abrupt fluctuations in wet and dry events, with the early and middle Holocene showing longer wet events than the late Holocene (from 4.0 kyr BP onwards) (Stríkis *et al*., 2011).

The present study aims to discuss how SASM variability has affected the fire activity and vegetation of the central Cerrados during the Pleistocene/Holocene transition and the early Holocene. Our discussion is based on a new high-resolution pollen, charcoal and XRF record from Lagoa Feia, which is located near Brasília in the core region of the Brazilian Cerrados. Lagoa Feia represents the first record from the central area of the Cerrados that covers the early Holocene, as previously published records from this region include hiatuses or no pollen record at the end of the Pleistocene and early Holocene (Salgado-Labouriau *et al*., 1997a; Barberi *et al*, 2000). The Lagoa Feia record provides unprecedented insight into landscape and rainfall variability in central Brazil. We have assessed the regional scope of these variations, along with their implications for SASM boundary belt oscillations based on comparisons with other pollen and paleoclimatic records from the Cerrados and adjacent regions.

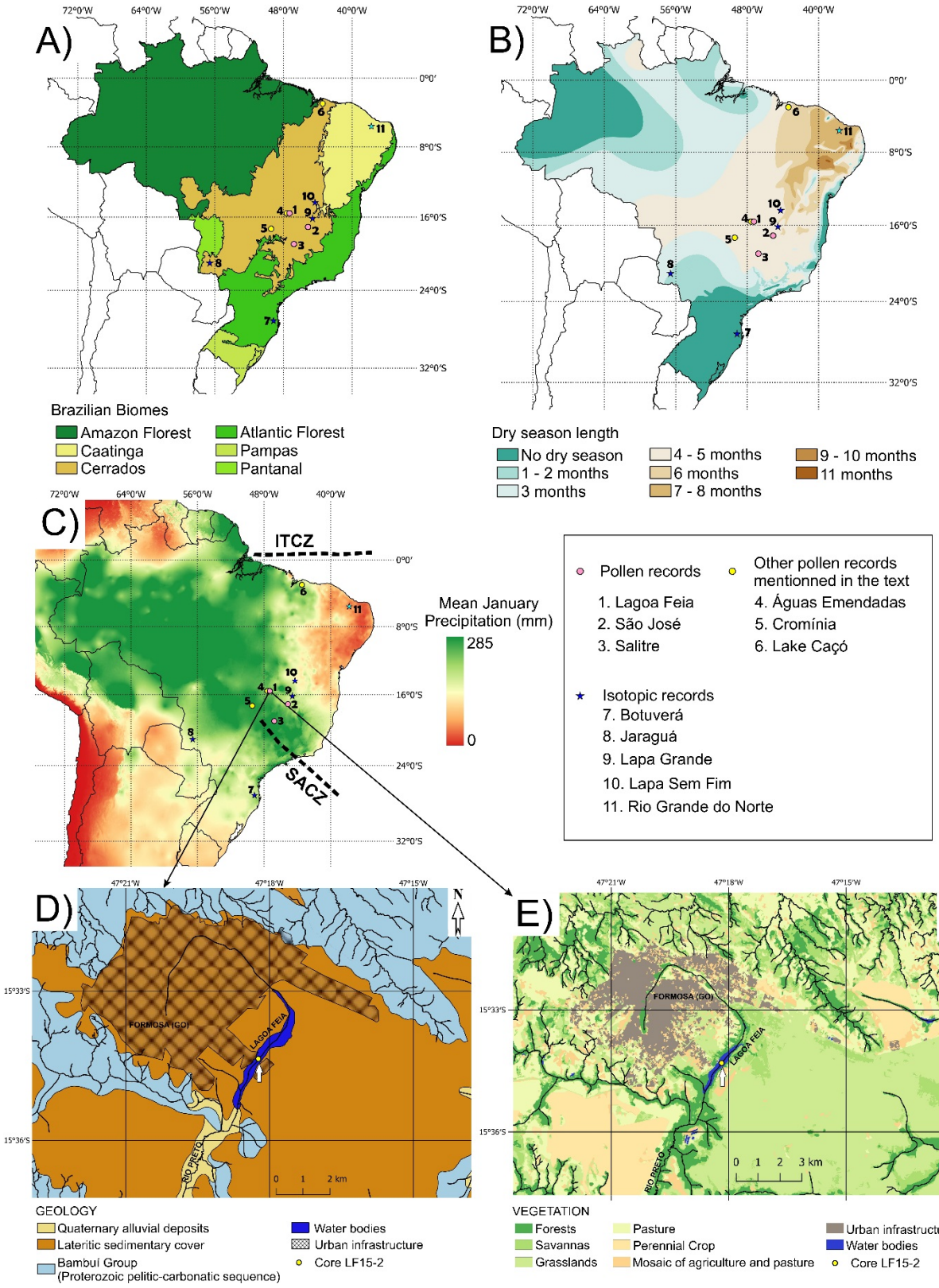


Figure 1: Geographic distribution and climate of the Cerrados, locations from which pollen (Lagoa Feia (this study); São José (Cassino *et al.*, 2018); Salitre (Ledru, 1993; Ledru *et al.*, 1996); Águas Emendadas (Barberi *et al.*, 2000); Cromínia (Salgado-Labouriau *et al.*, 1997); Lake Caçó (Ledru *et al.*, 2006)) and isotopic records (Botuverá (Cruz *et al.*, 2005; Wang *et al.*, 2007); Jaraguá (Novello *et al.*, 2017); Lapa Grande/Lapa Sem Fim (Stríkis *et al.*, 2015); Rio Grande do Norte (Cruz *et al.*, 2009)) mentioned in this study were collected, and geology and vegetation of the Lagoa Feia site. A) Distribution of Brazilian biomes (from IBGE, 2004); B) Map of the length of the dry season across Brazil (from IBGE, 2002); C) Mean January precipitation in South America during the apex

of the SASM season (from Fick & Hijmanns, 2017); D) Geological map of the region around Lagoa Feia (from Lacerda Filho *et al*., 2000); E) Vegetation map of the region around Lagoa Feia (from Project MapBiomas, 2019).

2. Vegetation and Climate in the Cerrados

The Brazilian Cerrados extends from the equatorial zone to around 24° south latitude in Central Brazil. As such, the Cerrados includes transitional areas with four other Brazilian biomes, namely, the Amazon Forest to the north, the Caatinga to the northeast, the Atlantic Forest to the east and the Pantanal to the west (Fig. 1A).

The Cerrados demonstrates high physiognomic diversity as the region includes forests, savannas and grasslands. The Cerrados contains two different kinds of forest formations: gallery, or riverine, forests that follow streams and rivers and the dry forests. The dense canopy of the gallery forests maintains constant moisture, even during the dry season; for this reason, the trees are usually tall and not deciduous, with Apocynaceae, Fabaceae, Lauraceae and Rubiaceae the most represented families (Ribeiro & Walter, 2008). The dry forests are mainly deciduous, occurring either on well-drained and nutrient-rich soils or more dystrophic soils. The most common tree species (e.g. *Caryocar brasiliense*, *Qualea grandiflora*) in dry forests are also found on savanna formations (Ribeiro & Walter, 2008).

The savanna formations (called Cerrado *stricto sensu*) have clearly delimited arboreal and shrubby-herbaceous strata (Ribeiro & Walter, 2008), with arboreal cover ranging from 5% (sparse Cerrado) to 50% (dense Cerrado). High floristic diversity is encountered on the Cerrado *stricto sensu*; for example, when Ratter *et al*. (1996) compared around 100 floristic surveys from this formation, they found that from a total of around 530 species only 26 (e.g. *Astronium fraxinifolium*, *Bowdichia virgiloides*, *Byrsonima coccolobifolia*, *Caryocar brasiliense*, *Roupala montana*, *Tabebuia aurea*) were identified in at least 50% of the surveys.

In addition, grassland formations, with Poaceae, Asteraceae and Cyperaceae the most represented families, are differentiated according to the presence or absence of a shrubby stratum.

The most remarkable feature of the climate of the Cerrados is rainfall seasonality (Fig. 1B). According to the Koppen criteria, most of the Cerrados region is classified as Aw, i.e. Tropical climate which includes a dry austral winter (Alvares *et al*., 2013) extending four to six months that is characterized by severe water deficiency. The rainy season starts in September-October and ends in March-April, with

its apex between November-January when around 50% of annual rainfall occurs (Fig. 1C) (Silva *et al*., 2008). The apex of the austral summer rainy season corresponds to the mature phase of the SASM, which occurs between November and February. During this time, deep convection occurs over Central Brazil (Vera *et al*., 2006). Total annual precipitation in most of the Cerrados ranges between 1,000 to 1,800 mm, but some areas in eastern Cerrados, especially those at the transition zone with Caatinga, receive only 400 to 600 mm of precipitation per year. On the other hand, more than 2,000 mm of annual precipitation has been registered in some areas of northwestern Cerrados (Silva *et a*l., 2008). Mean annual temperature in the Cerrados varies from 18-19°C in the southeast to 26-27°C in the northeastern area of the biome (Silva *et al*., 2008). Thermal amplitude between months in the Cerrados is relatively low, as the mean minimum temperature never falls below 14°C while the mean maximum temperature never exceeds 33°C (Silva *et al*., 2008).

3. Materials and Methods

3.1. Lagoa Feia record

3.1.1. Settings

Lagoa Feia is an elongated lake about 3 km long in the NE-SW direction and about 140 m wide. It is located in the city of Formosa (Goiás State), which is close to the Brazilian capital, Brasília. It is connected to a small drainage upstream and is the source of the Rio Preto (Fig. 1D). The water is about 5 m deep at the center of the lake, with aquatic plants currently covering a large part of the lake's surface.

Lagoa Feia is located on a plateau at an altitude of around 900 m that is composed of lateritic sedimentary soil that overlies a Proterozoic pelitic-carbonatic sequence of the Bambuí Group (Fig. 1D). The lake may have been formed through sub-superficial carbonate dissolution, which caused local subsidence of the plateau (Ferraz-Vicentini, 1999). The urban area of Formosa extends on the west side of the lake, while there is a very large (1,100 Km^2) uninhabited, preserved area belonging to the Brazilian Army on the east side of the lake. In this area, vegetation is composed of patches of grasslands and open savannas, with marshes present on depressed areas of the plateau (Fig. 1E). Forests occur along the drainage area and on the sloping hillsides downstream of Lagoa Feia.

Regarding climatic conditions, the Lagoa Feia region has a mean annual precipitation of around 1,500 mm, a mean maximum temperature of 26°C and a mean minimum temperature of 14°C (according to meteorological data for the last ten years, available on BDMEP/INMET - Instituto Nacional de Meteorologia (http://www.inmet.gov.br)).

3.1.2. Chronology, pollen, charcoal and XRF scanning

A 500-cm deep core, Core LF15-2, was collected from the center of Lagoa Feia, at 15°34'S, 47°18'W, with a Livingstone corer in 2015. A total of 24 samples from the upper 435 cm underwent radiocarbon dating by Accelerator Mass Spectrometry (Table 1) at the French *Laboratoire de Mesure du Carbone 14* (LMC14) – UMS 2572 (CEA/DSM, CNRS, IRD, IRSN, dates from bulk samples). The age-depth model was built with Bacon (Blaauw & Christen, 2011), using the calibration curve SHcal13 (Hogg *et al*., 2013) (Fig. 2), and with "boundaries" set at 415.5 and 437 cm; other parameters were kept as default.

Subsamples of 0.5 cm^3 taken about every 4 cm were prepared for pollen analysis using standard methods (eg. Bennet & Willis, 2001), including treatment with HF-40%, HCl-30%, KOH-10% and acetolysis. After each treatment, samples were centrifuged to concentrate the pollen grains; no sieving was used in the process so that palynomorphs of all sizes were retained. Spores of the marker *Lycopodium clavatum* (Stockmarr, 1971) were added prior to treatment for concentration calculations. Following analyses, 32 subsamples from a total of 111 subsamples presented very low pollen concentrations and were considered sterile. In the other samples, at least 300 terrestrial pollen grains - excluding aquatic and water-level-related taxa (e.g. Cyperaceae) - were counted. Pollen, spore and other palynomorph percentages were calculated relative to the terrestrial pollen sum. Pollen diagrams were plotted with C2 software (Juggins, 2007), and zonation was based on constrained hierarchical clustering that applied the Coniss method and included all terrestrial pollen taxa on the analysis. Pollen data from the Lagoa Feia record was compared with data from the Salitre (Ledru, 1993; Ledru *et al*., 1996) and São José (Cassino *et al*., 2018) pollen records to evaluate the regional significance of vegetation changes. New age-depth models were generated for these two cores with Bacon (Blaauw & Christen, 2011), using the calibration curve SHcal13 (Hogg *et al*., 2013; Supplementary Material Fig. 5-6). Pollen percentages were recalculated from pollen counts for the Salitre and São José records using as reference the terrestrial pollen sum.

Pollen data from the three sites were then summarized using four curves: % Grassland taxa (*Alternanthera*; Asteraceae; *Cuphea*; *Drosera*; Eriocaulaceae; *Galianthe*; Poaceae; *Xyris*); % Savanna taxa (*Astronium*-Type; *Borreria*-Type; *Byrsonima*; *Caryocar*; *Cupania*; *Forsteronia*-Type; *Matayba*; *Mimosa*-Type; Myrtaceae; *Plenckia*; *Richardia*; *Roupala*; *Sapium*; *Sebastiania*; *Senna*-Type; *Tabebuia*-Type; *Tapirira*-Type); % Forest taxa (*Alchornea*; *Anadenanthera*; *Hedyosmum*; Moraceae; *Myrsine*; *Sloanea*; *Symplocos*; *Trema*); and % cold-adapted taxa (*Drymis*, *Weinmannia*; *Araucaria*). To assess regional patterns of vegetation variability, a Principal Components Analysis (PCA) was performed using the % Grassland taxa, % Savanna taxa and % Forest taxa from the three cores. Prior to PCA, pollen data were interpolated to every 200 years (only considering non-sterile pollen samples) and square-root transformed.

Subsamples of 0.5 cm^3 taken every 2 cm were prepared for macro-charcoal analysis by treating them with NaOCl and KOH to concentrate charcoal particles. The subsamples were then sieved through 160 µm mesh and analyzed in the microscope to separate charcoal particles. WinSeedle software (Regent Instruments, Quebec, Canada) was used to count the particles and measure their size. Charcoal data are expressed as charcoal influx (number of particles/cm^2/year) and as charcoal area (charcoal total area/cm^2/year).

The entire core was subjected to XRF core scanning with a resolution of 0.5 cm at the *Laboratoire EDYTEM Université Savoie Mont-Blanc* - CNRS. Two runs were performed, with the settings of the first run adjusted at 10 kV to measure light elements (Al to Fe), while the settings of the second run were adjusted to 30 KV for heavier elements (Cu to Pb). Titanium, which is considered an unambiguous indicator of allochthonous input (Davies *et al*., 2015), was used to normalize other elements (Ca, Fe, S, Si, Sr, Zn) and discriminate in-lake mineral input.

4. Results for the Lagoa Feia record

4.1. Core sedimentology, XRF scanning results and chronology

Core LF15-2 demonstrated three distinct sediment layers: the sediment between 500-437cm was composed of fine to coarse siliciclastic sand, with clay content increasing towards the top of the layer; the

sediment between 437-415.5 cm was composed of black clay; while the sediment from 415.5 cm to the top of the core was mainly composed of organic sediment with vegetal fibers (Fig. 2).

The XRF core scanning results also revealed three main depositional units that corresponded to the three sedimentary layers. The XRF scanning results from the bottom to 437 cm indicated high Si content, along with relatively high K and Al contents (Unit 1, Fig. 3), which reflects the predominance of siliciclastic sand. The clay layer above this first depositional unit (Unit 2) was characterized by an increase in several lithogenic minerals (Zr, Rb, K, Al and Ti) as well as Fe and Ca; Si was not as noticeable in this layer as it was in the bottom layer. The organic layer (spanning from a depth of 415.5 cm to the top (Unit 3)) displayed decreased levels of all lithogenic minerals relative to the other layers, and high levels of S, Ca and Sr.

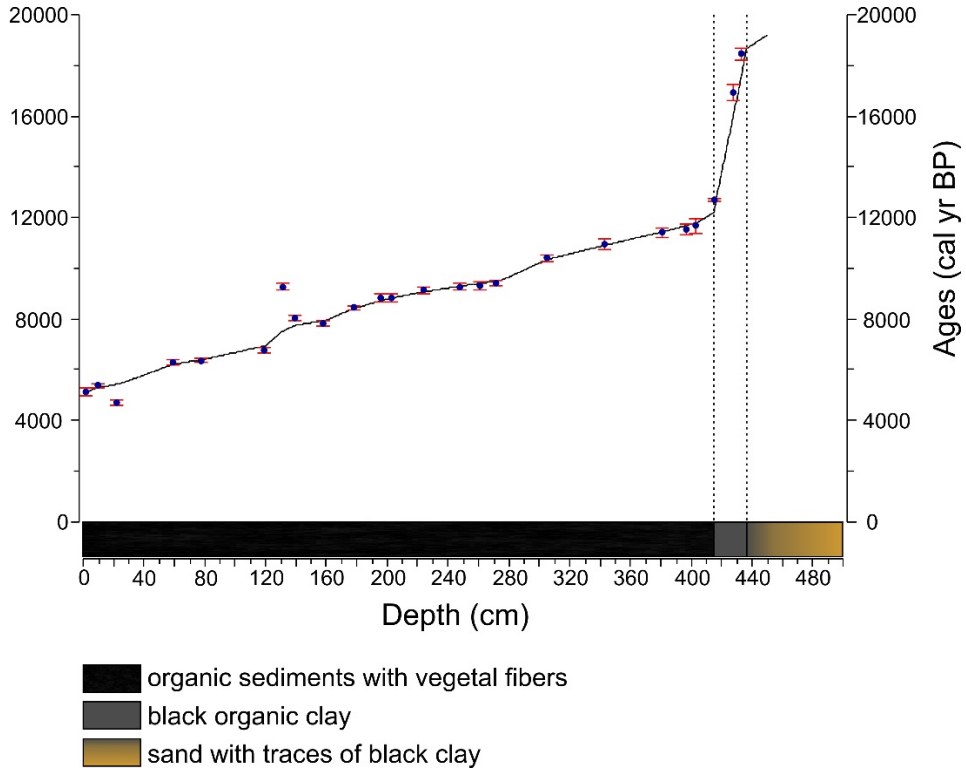


Figure 2: Lithology and age-depth model for the LF15-2 sediment core. Calibration intervals for ^{14}C dates are plotted in red. Boundaries for accumulation rate calculations were set at the thresholds between different sediment layers (vertical dashed lines).

These depositional units revealed three different stages of sedimentation in the Lagoa Feia basin. Unit 1 shows medium to high-energy deposition of detrital sediments, which was most probably related to alluvial deposition prior to lake formation. Unit 2 reflects conversion to low-energy sedimentation

characterized by detrital clay input, which marks the beginning of lacustrine deposition and the drowning of the valley. The low Ca/Ti, Si/Ti and Fe/Ti ratios in unit 2 relative to unit 3 suggest predominantly allochthonous mineral input, without significant contribution of in-lake production. In unit 3, the lacustrine deposition changes to autochthonous organic sedimentation, which explains the low levels of lithogenic elements observed in this unit. Relatively high Ca and Sr levels, along with high Ca/Ti and Sr/Ti ratios, in unit 3 suggest the presence of biogenic/authigenic in-lake carbonate deposition. The transition from unit 2 to unit 3 was gradual, and included a transitional phase during which fine detrital input progressively shifted to organic sedimentation.

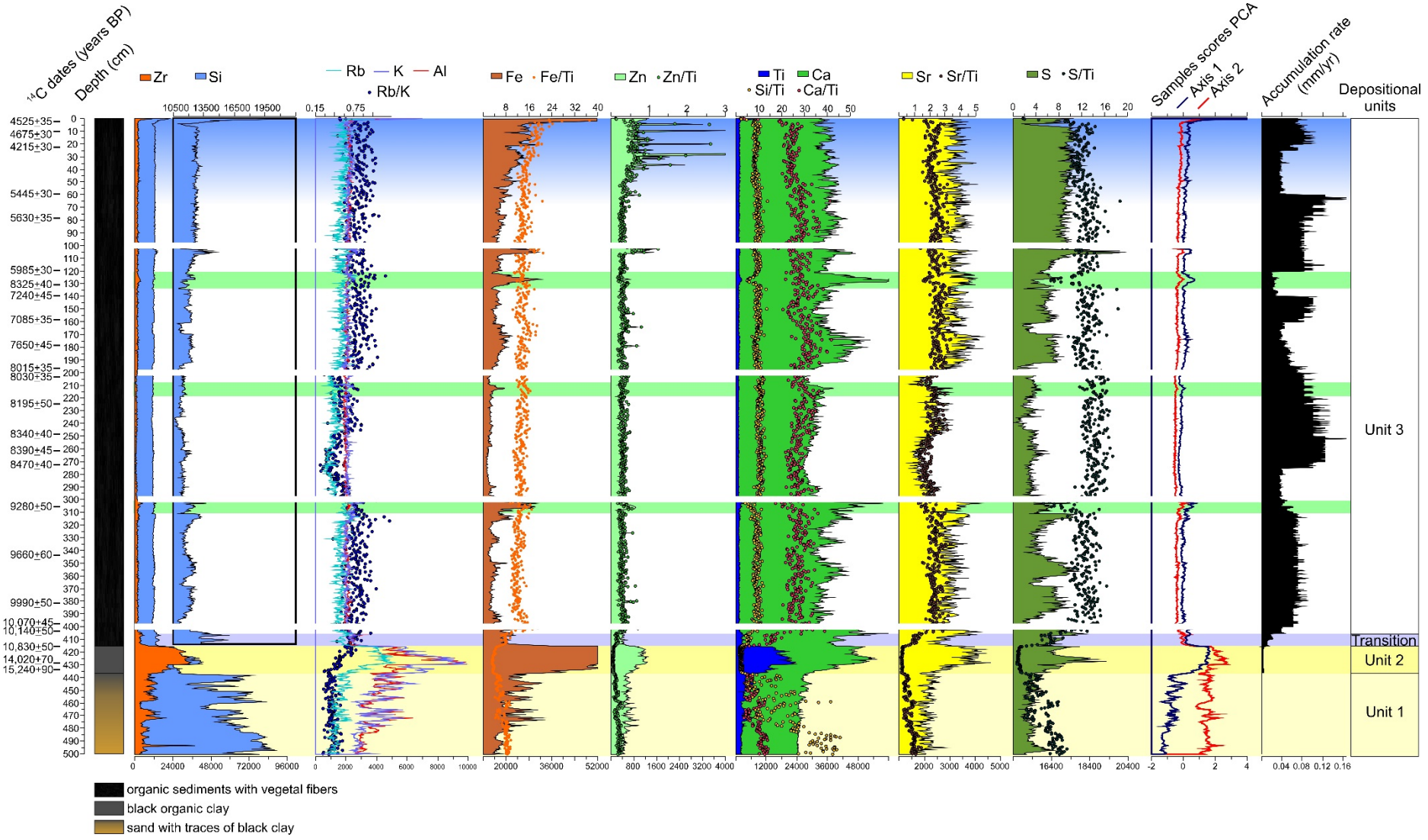


Figure 3: XRF scanning results showing the levels of selected elements (Zr, Si, Rb, K, Al, Fe, Zn, Ti, Ca, Sr, S), along with relevant ratios (Rb/K, Fe/Ti, Zn/Ti, Si/Ti, Ca/Ti, S/Ti), for core LF15-2 plotted against depth. Green bands highlight episodes of increase in Ti and Fe content during Unit 3. Radiocarbon ages are indicated on the left side. Samples scores for the two first axes of the PCA (Supplementary Material, Fig. 1) and accumulation rate curves are shown on the right side. XRF data at the junction of the core sections were disconsidered (white bands) because of possible edge-induced errors during the scan.

A PCA was performed with the most significant non-organic elements (Supplementary Material, Fig. 1). The PCA was able to differentiate the three main units of sedimentation. The results showed that Ca, Sr, Ni, S and Br were relatively more abundant in the organic sediments of unit 3 than in sediments representing the other units, while lithogenic elements Ti, Si, Zr, K and Al were correlated with samples from units 1 and 2. In unit 3, there were three episodes in which the content of Ti increased (shown by green bands in Fig. 3, and corresponding to decreased Ca/Ti); these episodes were also identified on the first axis of the PCA and could reflect time periods when organic deposition shifted to mineral input. These episodes were also associated with Fe peaks, which suggests that the lake sediments may have been exposed to oxidation as a result of lower lake levels during these periods.

Radiocarbon dates obtained for the upper 435 cm of LF15-2 (Table 1, Fig. 2) show an age of around 15,240 ^{14}C yr BP (~18,400 cal yr BP) at the bottom of the record and 5,525 ^{14}C yr BP (~5,100 cal yr BP) at the top. The two units with lacustrine deposition (units 2 and 3) showed distinct sedimentation rates on the age-depth curve. The clay layer (unit 2), between 436.5 and 415.5 cm, represents a 4,500 year interval and suggests very low sedimentation rates. The deposition of organic sediments (unit 3) is well constrained by twenty-two radiocarbon dates that indicate higher, and relatively constant, sedimentation rates during the early and middle Holocene. In the LF15-2 age-depth model (Fig. 2), boundaries constraining changes in the sedimentation rate were set at 415 and 437 cm to coincide with sedimentological changes.

Table 01: Radiocarbon dates of the LF15-2 core. Calibrated ages (two standard deviations (2σ) ranges) were obtained from Calib 7.0 (Reimer *et al*., 2013).

Lab Code	Depth (cm)	^{14}C yr BP	δ^{13}C	Age range (cal yr BP) 2σ
SacA47388	2	4525 ± 35	-26,8	4,976 - 5,297
SacA57452	10	4675 ± 30		5,300 - 5,467
SacA49368	22	4215 ± 30	-31,1	4,582 - 4,834
SacA49369	59	5545 ± 30	-25,2	6,215 - 6,397
SacA47389	78	5630 ± 35	-32	6,298 - 6,441
SacA49373	119	5985 ± 30	-25,7	6,673 - 6,879
SacA57453	131	8325 ± 40		9,131 - 9,426
SacA47393	139	7240 ± 45	-27,6	7,939 - 8,158
SacA49374	158	7085 ± 35	-27,7	7,792 - 7,955
SacA47394	178	7650 ± 45	-26,1	8,343 - 8,536
SacA49375	196	8015 ± 35	-27,4	8,651 - 8,996
SacA49370	203	8030 ± 35	-29,9	8,660 - 9,003
SacA47390	224	8195 ± 50	-20,8	9,001 - 9,264
SacA49371	248	8340 ± 40	-29,1	9,137 - 9,432
SacA47391	261	8390 ± 45	-25,4	9,149 - 9,483
SacA49372	272	8470 ± 40	-29,1	9,314 - 9,529
SacA47395	305	9280 ± 50	-25,9	10,255 - 10,552
SacA47396	343	9660 ± 60	-21,6	10,756 - 11178
SacA48900	381	9990 ± 50	-29,9	11,239 - 11,613
SacA49376	397	10070 ± 45	-29,5	11,313 - 11,756
SacA47398	403	10140 ± 50	-30	11,397 - 11,958
SacA49377	415	10830 ± 50	-24,4	12,659 - 12,753
SacA47399	428	14020 ± 70		16,640 - 17,224
SacA57454	433	15240 ± 90	-22	18,226 - 18,691

4.2. Pollen and charcoal

A total of 155 pollen types were identified from LF15-2 samples (Table 1, Supplementary Material), plus 12 types of spores and other palynomorphs (algae zygospores, zooclasts, "Tintinomorphs" and leaf spines of *Ceratophyllum*). Pollen analysis was performed on the upper 445 cm of the core, i.e., this analysis included the top of depositional unit 1 and units 2 and 3. Pollen concentrations varied noticeably between the units (Fig. 4). The clay layer (unit 2) was characterized by a low sedimentation rate (around 0.003 mm/yr) and showed very high pollen concentrations (around 100,000 grains/cm³), while most samples from the organic sediments of unit 3 showed comparatively lower pollen concentrations (usually less than 20,000 grains/cm³). This may be explained by the high sedimentation rate of unit 3 (maximum of 0.16mm/yr).

A cluster analysis that included terrestrial pollen types identified five pollen zones (Fig. 4):

i) Zone LF01 (445-421 cm; ca 19,000 to 14,400 cal yr BP; 7 samples)

This pollen zone corresponds to the top of depositional unit 1 and most of depositional unit 2. Samples showed high frequencies of Poaceae (max. 53%) and marsh plants (*Cuphea* (max. 2.3%), *Xyris* (max. 5%) and *Eryngium* (max. 2%)), as well as high frequencies of Bryophytes (*Phaeoceros* and *Sphagnum*) and *Lycopodiella* (Supplementary Material, Fig. 4). These samples showed relatively low frequencies of Cyperaceae, ferns, and algae. Furthermore, zygospores from *Debarya* were restricted to this zone. Zone LF01 also had high frequencies of

Asteraceae (max. 26.2%), while arboreal forest taxa were represented by *Hedyosmum* (max. 4.9%), *Ilex* (max. 2.9%) and *Myrsine* (1.7%). The cold-adapted taxa *Weinmannia* and *Drimys* were also present (Supplementary Material, Fig. 2). Charcoal was not detected from this zone (Fig. 5).

ii) Zone LF02 (417-405 cm; ca 13,300 to 11,850 cal yr BP; 4 samples)

Zone LF02 corresponds to the transitional zone between depositional units 2 and 3 (Fig. 4), and differs from the previous zone in that it had lower frequencies of Poaceae (< 18%) and marsh plants, and higher frequencies of forest taxa, with the appearance of new arboreal taxa such as *Banisteriopsis*-Type (Malpighiaceae - max. 31%), Moraceae (1%), as well as Annonaceae, *Serjania*, *Prunus* and *Dendropanax* (Supplementary Material, Fig. 2-4). Charcoal was detected from the top of the zone (0.9 particles/cm²/yr) (Fig. 5).

iii) Zone LF03 (401-363 cm; 11,800 to 11,190 cal yr BP; 11 samples)

This zone showed clear Cyperaceae (72%) and *Blechnum*-Type (88%) peaks. Spores from two other fern genera, *Acrosthicum* and *Osmunda*, also showed high frequencies in this zone (Supplementary Material, Fig. 4), while the presence of Bryophytes, *Lycopodiella* and marsh plants has almost disappeared. Aquatic plants (Pontederiaceae) peaked (11%) at around 11,500 cal yr BP, and then become rare. Poaceae showed alternating frequencies, with very high (45%) and low (less than 5%) values. This zone also marks the start of samples with high frequencies of *Gomphrena*. This taxon also shows alternating frequencies, with both high and low values observed throughout the zone. When compared to the previous zone, this zone demonstrates an important change in local vegetation. The forest assemblage observed in the previous zones (comprising *Hedyosmum*, *Ilex*, *Myrsine, Banisteriopsis*-Type and *Weinmannia)* shifts to other arboreal forest taxa such as *Anadenanthera* (max. 3.6%), Moraceae (max. 14%), *Celtis* (max. 2.4%), and *Doliocarpus* (max. 4%), as well as *Trema* and *Schefflera* (Supplementary Material, Fig. 4). The arboreal species *Erythrina* (max. 5.8%) was exclusively identified from this zone. Typical Cerrado arboreal taxa *Byrsonima* (max. 4%) and *Astronium*-Type (max. 7.5%) became more abundant in this zone, which also showed isolated presence of *Caryocar*, *Plenckia* and *Forsteronia* (Supplementary Material, Fig. 2-4). Charcoal was present in this zone, although showed low influx (maximum value of 1.8 particles/cm²/yr) (Fig. 5).

iv) Zone LF04 (359-121 cm; 11,140 to 7,000 cal yr BP; 60 samples)

Most of the sterile samples identified from the core were concentrated in Zone LF04. These 23 sterile samples were intercalated with 37 pollen-rich samples (more than 20,000 grains/cm³). *Botryococcus*, Cyperaceae, Poaceae and *Gomphrena* showed alternating high and low frequencies throughout the zone. The zone showed lower frequencies of arboreal pollen than the previous zone, and some arboreal forest taxa (e.g. Moraceae, *Doliocarpus*) were either no longer present or had become rare. *Astronium*-Type (0 to 11.3%), *Anadenanthera* (0 to 6.4%) and *Byrsonima* (0 to 6%) occurred at irregular frequencies. Two peaks of high charcoal influx were identified from the bottom of this zone, centered at around 11,000 and 10,600 cal yr BP (6.0 and 1.9 particles/cm²/yr, respectively) (Fig. 5).

v) Zone LF05 (117-01 cm; 6,900 to 4,980 cal yr BP; 29 samples)

Zone LF05 showed an abundance of *Ceratophyllum* (an aquatic submerged plant) leaf spines (max. 15%) and an increase in the frequency of *Zygnema* zygospore. Furthermore, two aquatic plants that were not observed in the previous zone, *Sagittaria* and Nymphaeaceae, were found in this zone (Supplementary Material, Fig. 2-4). From a depth of 51 cm to the top, the pollen content between samples became less irregular and arboreal taxa such as *Astronium*-Type (max. 6.4%), *Anadenanthera* (max. 6,7%) and *Celtis* (max. 2.3%) showed constant frequencies. Zone LF05 also showed more continuous charcoal influx (Fig. 5), with peaks at 6,750; 6,650 and 5,100 cal yr BP (2.3; 1.4 and 5.8 particles/cm²/yr, respectively).

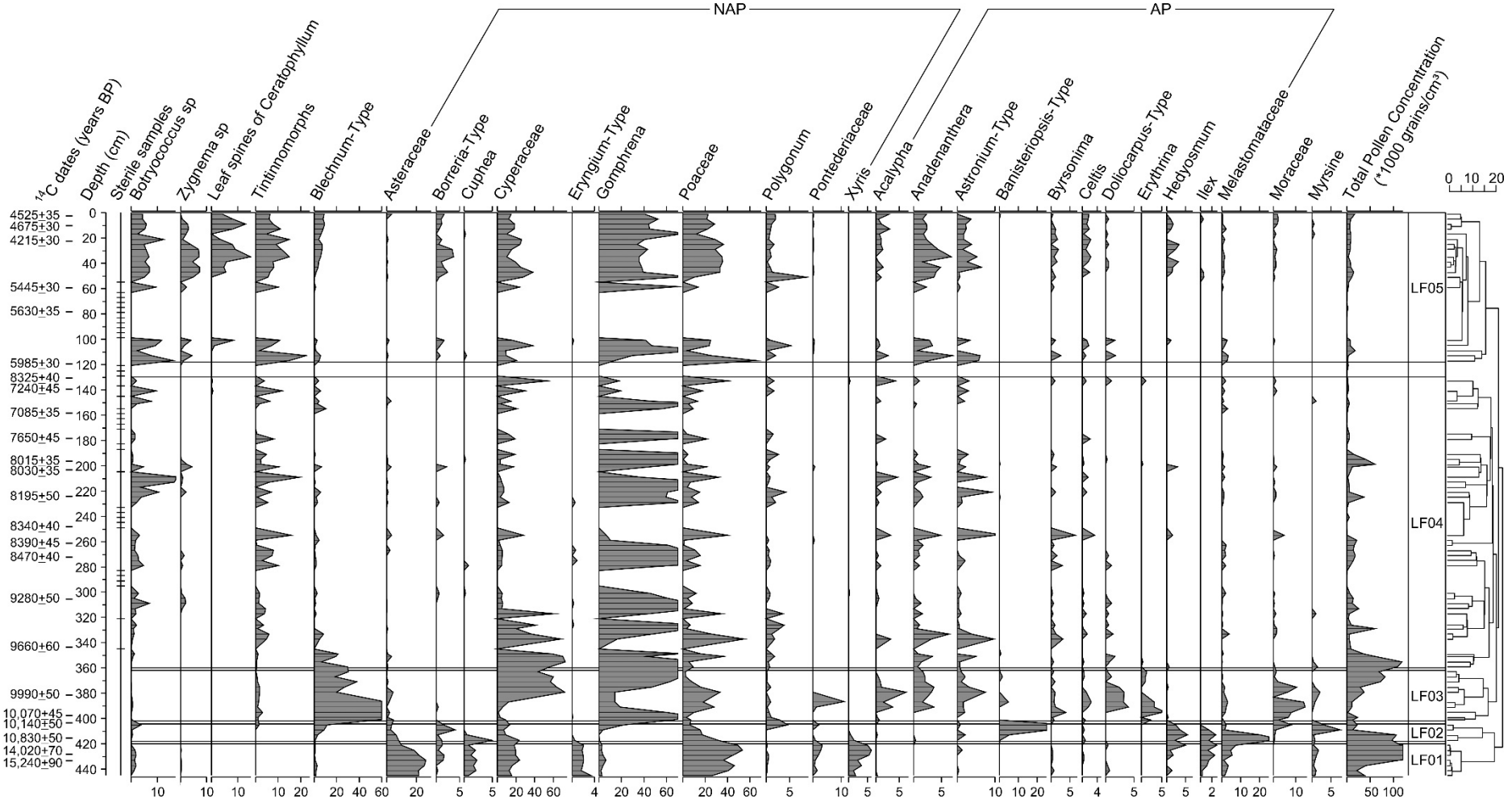


Figure 4: Synthetic pollen percentage diagram for the LF15-2 core, with data plotted against depth (y-axis). Radiocarbon dates, positions of sterile samples, the frequency of 28 selected non-pollen palynomorphs (NPP), non-arboreal pollen (NAP) and arboreal pollen (AP), pollen concentrations, pollen zones and a cluster dendrogram are shown (from left to right). For a complete diagram, please refer to the Supplementary Materials – Fig. 2-4.

330 **5. Discussion**

331 **5.1. Paleoecological interpretation of the Lagoa Feia record**

332 The observed changes in the geochemical, pollen and charcoal aspects of the Lagoa Feia record describe
333 significant changes in lake, vegetation and fire regime dynamics.

334 Lacustrine deposition at Lagoa Feia began around 19,000 cal yr BP, right after the Last Glacial Maximum
335 (21 to 19 kyr). Lake formation could be explained by local subsidence of the plateau due to sub-superficial
336 limestone dissolution associated with superficial weathering (Ferraz-Vicentini, 1999). These processes would have
337 raised the groundwater table to the surface, which then subsequently drowned the valley and established a
338 source for the downstream Rio Preto river. In Late Pleistocene, until ~13,300 cal yr BP (depositional unit 2 and
339 pollen zone LF01), the very low sedimentation rate of fine sediment and the high content of marsh plants (Fig. 5),
340 Bryophyte and *Lycopodiella* suggest the formation of a shallow lake surrounded by marshes. The high frequencies
341 of Asteraceae and Poaceae indicate an open landscape around Lagoa Feia at that time. The arboreal taxa present
342 in this zone (*Hedyosmum*, *Ilex*, *Myrsine*) are consistent with the presence of gallery forest (Fig. 5). The presence of
343 *Weinmannia* and *Drymis* (Supplementary Material, Fig. 2), which are cold-adapted taxa, along with *Hedyosmum-*
344 *Ilex-Myrsine,* suggests that the climate was colder during this period than it is currently. However, the low
345 sedimentation rates noted for this period, which could also be due to depositional hiatuses, imply that the late
346 Pleistocene is not represented in detail on the Lagoa Feia record.

347 Higher temporal resolution started around 12,300 cal yr BP, which corresponds to a transitional phase
348 towards more organic sedimentation. This change in sedimentation is interpreted to reflect an increase in lake
349 levels. Organic matter originating from algae, ferns and aquatic plants would have been preserved by prevailing
350 anoxic conditions at the lake bottom. The transitional phase detected by XRF scanning corresponds to pollen zone
351 LF02, which showed decreased frequencies of marsh plants and Bryophytes, increased frequencies of *Polygonum,*
352 and the appearance of Tintinomorphs at the top of this zone (Fig. 5). All of these findings are consistent with the
353 transition to a deeper lake environment.

354 Following the transitional phase, a deeper, lacustrine environment is fully established at the beginning of
355 depositional unit 3 (around 11,900 cal yr BP). Cyperaceae and *Gomphrena* (Amaranthaceae) are the most
356 dominant taxa throughout depositional unit 3, and are probably related to local pollen production on the lake

margin. Cyperaceae pollen was not differentiated at the genus level, but two types of Cyperaceae pollen were dominant: a smaller pollen type, probably related to *Cyperus;* and a very large pollen type, possibly related to *Eleocharis* (Willard *et al*., 2004; Pollen collection ISEM). Both genera include amphibious and aquatic plants that colonize bogs, lakes and river margins in the Cerrados (Oliveira *et al*., 2011). Gomphrena, on the other hand, is present in the Cerrados as a herbaceous plant that occurs alongside Poaceae and Cyperaceae on humid or dry soils in open areas (Marchant *et al*., 2002; Fank-de-Carvalho *et al*., 2010). The occurrence of fire favors *Gomphrena* seed dispersal and germination (Fank-de-Carvalho *et al*., 2015), thus these plants tend to proliferate after the passage of fire (Fank-de-Carvalho *et al*., 2010). Therefore, the predominance of Cyperaceae over *Gomphrena* throughout unit 3 can be interpreted as lacustrine expansion, while samples in which *Gomphrena* frequencies exceeded Cyperaceae frequencies indicate periods characterized by temporary drying of parts of the lake and colonization by herbaceous plants. Although unit 3 represents a rise in lake levels when compared to the previous phase, lake levels were lower than they are now, as well as subject to temporary drying.

The increased lake levels observed during the transition to depositional unit 3 also coincide with the development of a more forested landscape. Arboreal pollen was more frequent and diverse in pollen zones LF02 and LF03 (i.e. between 12,500 - 11,190 cal yr BP) than in pollen zone LF01, suggesting the expansion of forests and/or arboreal savannas, which were previously limited to streams margins, on the plateau. *Erythrina*, restricted to pollen zone LF03, is associated with a tree that grows on moist habitats and is adapted to periodical flooding (Medina *et al*., 2009); thus, its presence suggests that a forest was also growing around the lake. Ecological observations of the present-day vegetation of the Cerrados indicate that the degree of arboreal cover is highly influenced by soil moisture. For instance, in a study of the association between Cerrados physiognomies and soil characteristics, Assis *et al*. (2011) showed that soil water availability is the main factor explaining the gradient from open savannas to woodlands when soil fertility is held constant. In another study, Terra *et al*. (2018) analyzed how several environmental factors were linked to the vegetation of 158 sites in Minas Gerais state (central Brazil). Their results demonstrated that soil water availability is the main factor driving tree density in these sites. Therefore, the increase in arboreal cover at Lagoa Feia observed in pollen zones LF02 and LF03 – which are also periods of rising lake levels – could have resulted from increased soil moisture, which is directly influenced by rainfall amount, the main factor underlying groundwater recharge (Cabral *et al*., 2015). These

pollen zones temporally coincide with the Younger Dryas event that can therefore be considered a wet period at the Lagoa Feia site.

From around 11,140 to 7,000 cal yr BP (LF04), gallery and moist forest taxa were less abundant around Lagoa Feia (Fig. 5), suggesting a more open landscape. The discontinuous presence of arboreal Cerrado and dry forest taxa, showed by a succession of high and low frequencies, indicates the repeated growth and decline of arboreal cover. This early Holocene period was also characterized by fluctuations in lake levels, with support coming from the predominance of *Gomphrena* over Cyperaceae, the presence of sterile samples, and episodes of increased mineral input. This suggests that the early Holocene (LF04) was drier than the Younger Dryas (LF02 and LF03), but included a series of centennial-scale moisture oscillations.

The onset of these drier conditions coincides with a period of high charcoal influx peaks between 11,000-10,600 cal yr BP (Fig. 5). The occurrence of fires at the beginning of the Holocene might have played a role in the decreasing forest cover observed around Lagoa Feia at that time. Studies based on modern observations suggest that the occurrence of fire significantly influences the degree of arboreal cover in the Cerrados, as frequent fires favor the development of an herbaceous stratum at the expense of a woody layer (Moreira, 2000; Durigan & Ratter, 2016). Fires in the Cerrados are almost exclusively surface fires - crown fires are not common – which burn the aboveground parts of herbs and grasses (Miranda *et al*., 2010). However, the ashes produced during these fires are deposited on the soil surface, providing nutrients that are readily absorbed by the shallow roots of grasses. As such, fires represent a transfer of nutrients from woody species to grasses (Oliveras *et al*., 2013). Furthermore, herbaceous species commonly have underground nutrient-storing organs, and the plants transfer nutrients belowground at the beginning of the dry season in a bid to survive fires that can only affect the nutrient-poor aboveground parts (Oliveras *et al*., 2013). Although some arboreal species of the Cerrados show fire adaptations (Sato *et al*., 2010), tree recruitment is overall negatively affected by fires (Mistry, 1998).

Apart from the peaks at the beginning of zone LF04, charcoal accumulation was not abundant during the early Holocene dry period. The low frequency of fires during this relatively drier phase could be due to a different pattern of annual rainfall distribution. Natural fires in the modern Cerrados are triggered by lightning and occur during the wet season or during the transitional months between seasons (Ramos-Neto & Pivello, 2000; Medeiros & Fiedler, 2004; Fiedler *et al*., 2006). Although lightning and natural fires were observed to be more frequent

411 during the wet season, these fires are quickly extinguished by subsequent rain and only burn small areas (Ramos-
412 Neto & Pivello, 2000). Natural fires occurring in September, which represents the transition from the dry to the
413 rainy season, burn significantly larger areas because at this time vegetation - which is still affected by the severe
414 water deficit from the dry season – offers plenty of dry fuel (Ramos-Neto & Pivello, 2000); these types of fires
415 have the most significant impact on vegetation (Miranda *et al*., 2010). The absence of sparse rains during the
416 transition phase between seasons could explain the relatively low occurrence of fires during most of the early
417 Holocene.

418 From around 6,900 to 5,000 cal yr BP, the presence of *Ceratophyllum* and a decrease in *Gomphrena*
419 frequencies suggest relatively higher, and more stable, lake levels. Furthermore, arboreal vegetation
420 representative of both moist and dry forests has a steadier presence around the lake (Fig. 5). Nevertheless, the
421 pollen record suggests that the studied region had less forests in this time period than during the wet period of
422 the Younger Dryas (LF02 and LF03). Pollen zone LF05 demonstrated high charcoal influx with almost all of the
423 samples including charcoal particles and high peaks observed in the beginning and towards the end of the phase.
424 The increased fire occurrence might have been linked to higher fuel availability and/or multiple rain events during
425 the transition between dry and wet seasons. Alternatively, the growing human populations in Central Brazil at the
426 time (Klink & Moreira, 2002) might have played a role in the increased fire frequency.

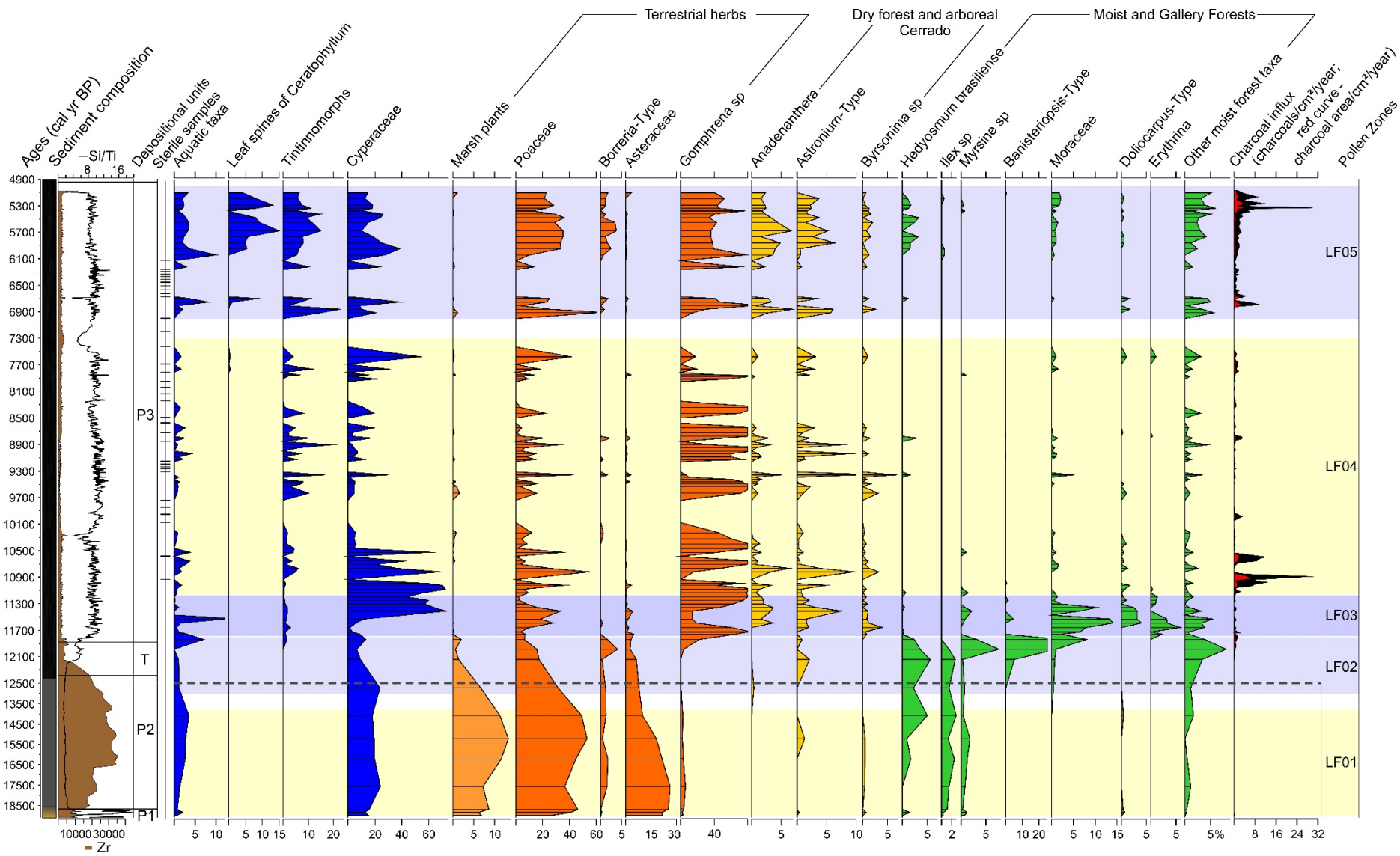


Figure 5: Summary pollen diagram for the LF15-2 core, with the data plotted against time (cal yr BP). Sediment composition, Zr levels, Si/Ti ratio and depositional phases are shown on the left. Background colors separate the five pollen zones (shown on the right); light yellow and shades of blue indicate drier and wetter phases, respectively. The bottom part of the core - below the dashed horizontal line - has a compressed time scale.

5.2. Central Brazilian Cerrados during the Pleistocene-Holocene transition and early Holocene

To test the regional scope of the paleoecological interpretation of the Lagoa Feia record, we compared our results with pollen records from the São José palm swamp (17°04'S, 45°06'W) (Cassino *et al*., 2018), located around 300 km to the southeast, and the Salitre bog (19°S 46°46'W) (Ledru, 1993), located around 400 km to the south (Fig. 6).

The Lagoa Feia and São José sites showed similar trends of vegetation cover and charcoal influx between 15 and 5 kyr BP, while the Salitre site for the same period showed an anti-phased trend. Between 12,700 and 11,200 cal yr BP, the Lagoa Feia and São José sites showed an increase in forest taxa frequencies, while the Salitre site, which is further south from the other two locations, showed a decrease in the frequencies of forest taxa (Fig. 6). São José showed relatively high frequencies of *Mauritia flexuosa* during this time period, which indicates the expansion of the palm swamp. During the early Holocene and beginning of the middle Holocene (~11,200 - 7,300 cal yr BP), an opposite trend was observed: at the Lagoa Feia and São José sites, forest taxa and arboreal savanna taxa, as well as *Mauritia flexuosa* at the São José palm swamp, were not as abundant as before, while the Salitre record revealed an increase in forest taxa, including the cold-adapted taxa *Drymis* and *Araucaria*. Subsequently, the Lagoa Feia and São José records showed a general trend of increasing arboreal taxa and *Mauritia flexuosa* frequencies between ~7,000 - 5,000 cal yr BP, while the Salitre site showed generally low forest taxa frequencies during this time period (Fig. 6).

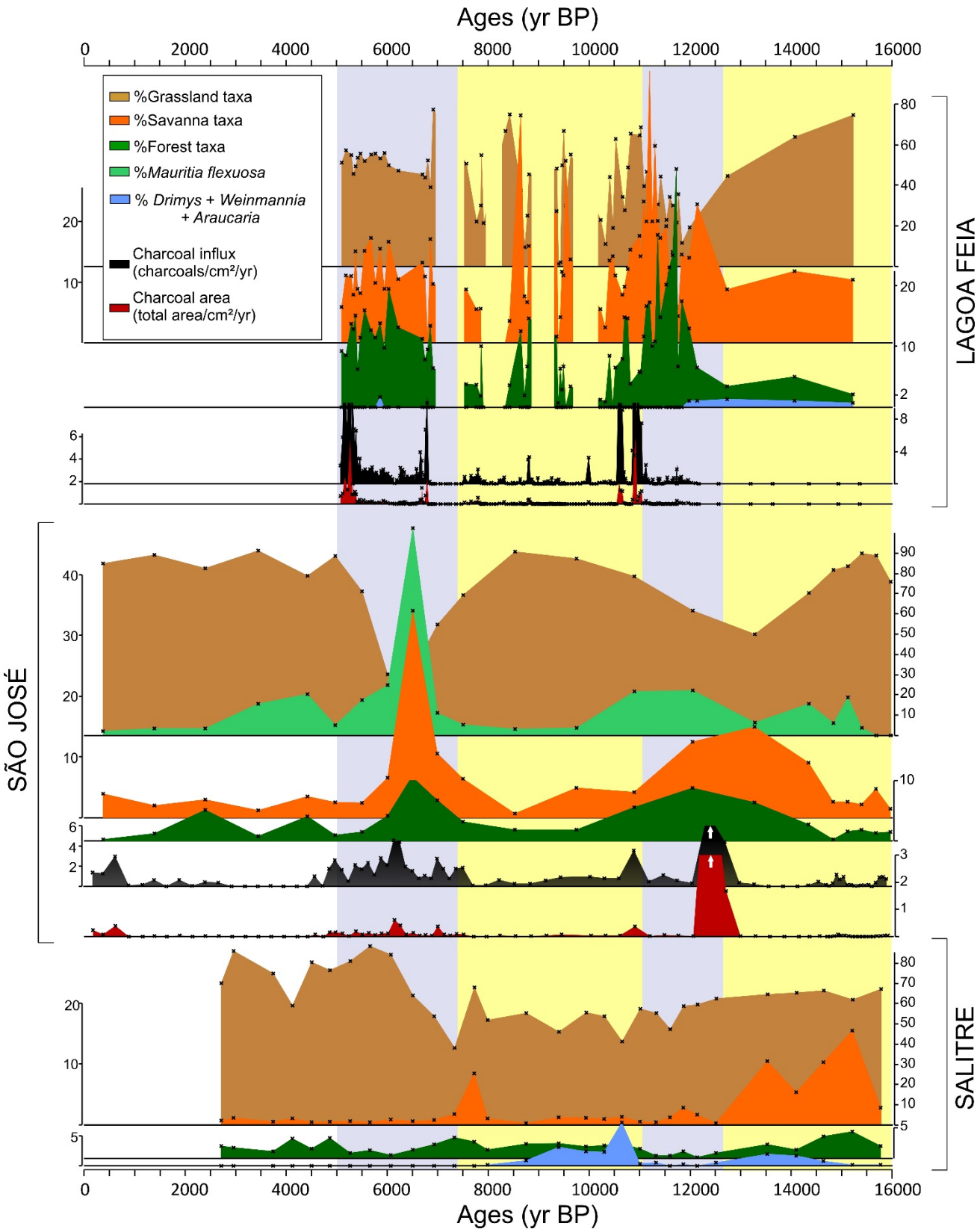


Figure 6: Synthetic representation of paleoecological changes over the last 16,000 years observed from the Lagoa Feia (this study), São José and Salitre cores (from Cassino *et al*., 2018 and Ledru, 1993, respectively). Grassland, savanna and forest include the following taxa: % Grassland taxa - *Alternanthera*, Asteraceae, *Cuphea*, *Drosera*, Eriocaulaceae, *Galianthe*, Poaceae, *Xyris*; % Savanna taxa - *Astronium*-Type, *Borreria*-Type, *Byrsonima*, *Caryocar*, *Cupania*, *Forsteronia*-Type, *Matayba*, *Mimosa*-Type, Myrtaceae, *Plenckia*, *Richardia*, *Roupala*, *Sapium*, *Sebastiania*, *Senna*-Type, *Tabebuia*-

Type, *Tapirira*-Type; and % Forest taxa - *Alchornea*, *Anadenanthera*, *Hedyosmum*, Moraceae, *Myrsine*, *Sloanea*, *Symplocos*, *Trema*.

This opposite trend between sites, i.e. forest expansion at the Lagoa Feia and São José sites synchronic to forest regression at the Salitre site and vice-versa, is visible in the first axis of the Principal Components Analysis of interpolated pollen data (PC1; Fig. 7). Time slices in which forest and arboreal savanna frequencies were high at the Lagoa Feia and São José sites and grassland taxa frequency was high at the Salitre site (between 13,200-11,200 cal yr BP and 7,000-5,600 cal yr BP) showed negative PC1 scores. For the early-middle Holocene (~11,000-7,000 cal yr BP), time slices were characterized by high frequencies of forest taxa at the Salitre site and high frequencies of grassland taxa at the Lagoa Feia and São José sites, and showed positive PC1 scores.

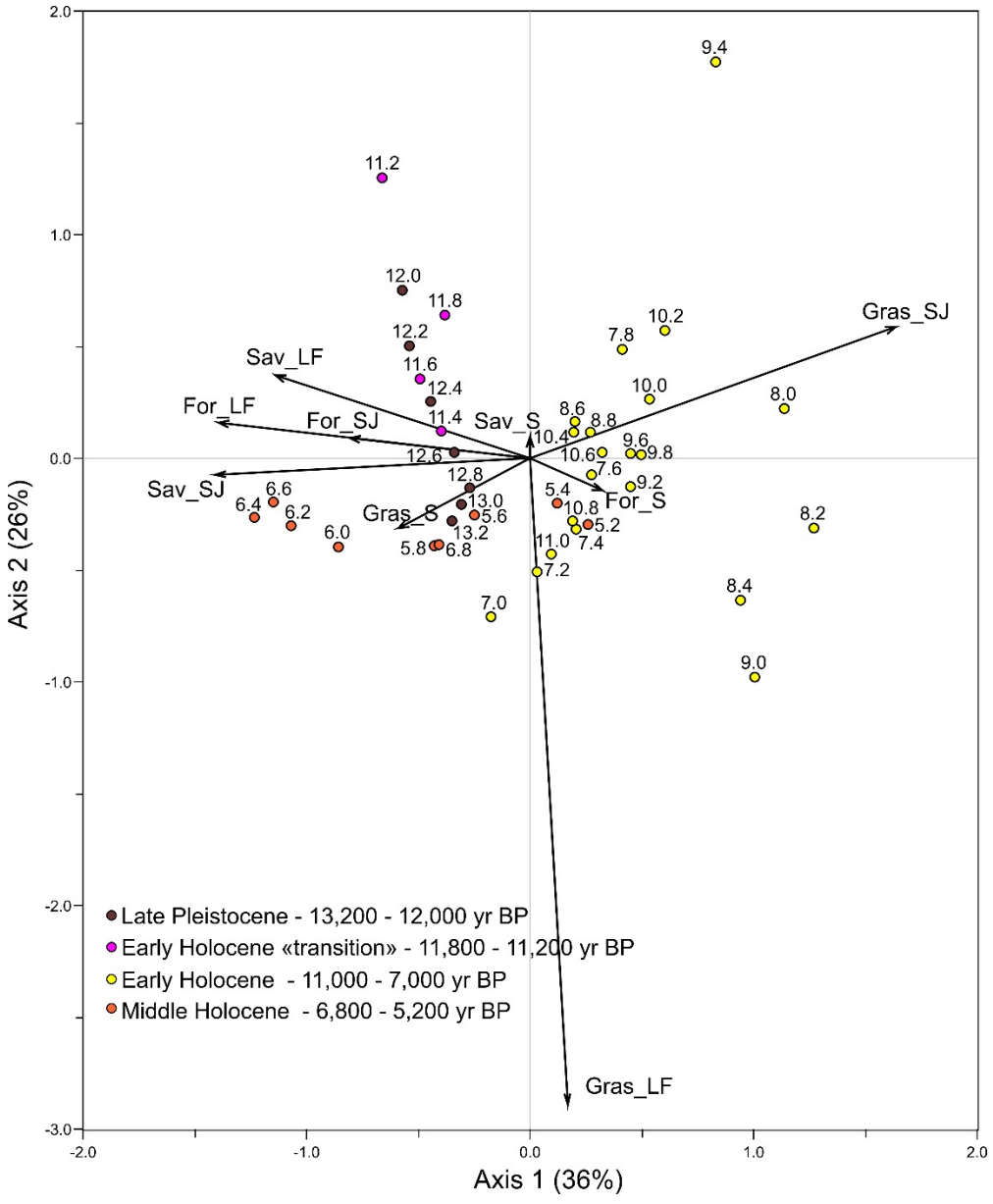


Figure 7: Principal Components Analysis of interpolated pollen data from Lagoa Feia, São José and Salitre records. Sample labels refer to ages in kyr BP. Species labels: Gras: % Grassland taxa; For: % Forest taxa; Sav: % Savanna arboreal taxa; LF: Lagoa Feia; S: Salitre; SJ: São José.

Charcoal records from Lagoa Feia and São José showed several common trends during the early and middle Holocene (Fig. 6). Peaks of high charcoal influx were detected from both cores at the beginning of the early Holocene, around 11,000 cal yr BP, although this was only detected from one São José sample. The São José record also showed very high charcoal influx around 12,500 cal yr BP, but the charcoal particles in these samples were noticeably larger than the particles from other samples (Fig. 6). This suggests that this peak represents a local fire that had reached the palm swamp border, from where the core was collected. Both records showed relatively low charcoal influx during most of the drier early-middle Holocene (11,000-7,000 cal yr BP), and higher charcoal influx during the relatively wetter middle Holocene (7,000-5,000 cal yr BP). The similarities in vegetation cover and charcoal influx between the Lagoa Feia and São José records support regional climatic control on arboreal cover and fire variability in central Cerrados during the Pleistocene-Holocene transition, while the contrasting trend for vegetation in the Salitre record indicates that different climatic processes affected the southern areas of this region.

5.3. SASM in central Brazil during the Pleistocene-Holocene transition and early Holocene

SASM variability in the central Cerrados during the Pleistocene-Holocene transition and early Holocene can be assessed by comparing vegetation cover variability in the central Cerrados, represented by the PC1 scores (Fig. 7) curve, with $\delta^{18}O$ speleothem records from adjacent regions (Fig. 8). During the Younger Dryas event (~13,000-11,200 cal yr BP), increased arboreal cover at Lagoa Feia and São José, shown by the PC1 scores curve and indicative of wetter conditions, correlates with more pronounced SASM activity in southern (Botuverá - Cruz *et al*., 2005; Wang *et al*., 2007), central-eastern (Lapa Sem Fim - Stríkis *et al*., 2015) and central-western (Jaraguá - Novello *et al*., 2017) Brazil (Fig. 8). This suggests that there was increased monsoon activity over a large area at that time (Fig. 9). The increase of monsoon activity in central South America during the Younger Dryas correlates with a dry episode in Northearsten Brazil (Fig. 8A; Cruz *et al*., 2009), and in northern South America (Haug *et al*., 2001; Maslin *et al*., 2011) which can be interpreted as a result of southward shifts in the ITCZ (Lea *et al*., 2003) and the SACZ (Cruz *et al*., 2005). Our results show that this area of stronger monsoon activity included central Brazil. This disagrees with previously studied pollen records from the Cerrados region (Salgado-Labouriau *et al*.,

1997a; Barberi *et al.*, 2000), in which the lack of deposition was interpreted as continuous aridity from the LGM to the Holocene. The curve representing vegetation variability in central Cerrados shows some delay in the timing of the end of this wetter phase in comparison to the δO^{18} records from Jaraguá and Botuverá (Fig. 8B and 8DC); there is no data for the end of the Younger Dryas in the Lapa Grande/Lapa Sem Fim record (Fig. 8C). This could reflect either an artefact from the interpolation of low-resolution pollen data or a delayed response (around 200 years) of vegetation to a changing climate.

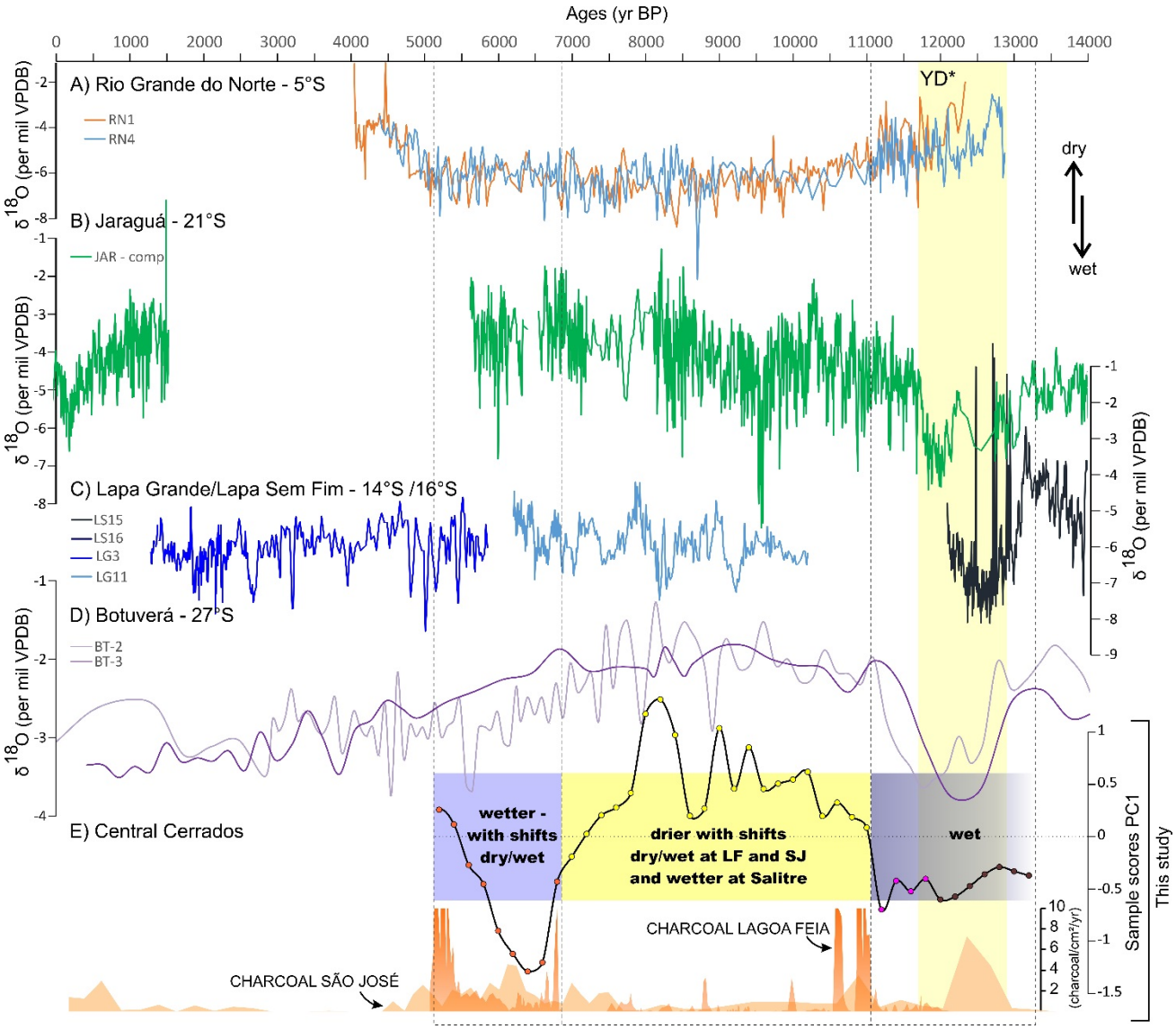


Figure 8: Comparison of vegetation cover variability in central Cerrados and δO^{18} speleothem records from adjacent regions. A) δO^{18} speleothem record from Rio Grande do Norte (5°S) (Cruz *et al.*, 2009); B) δO^{18} speleothem record from Jaraguá (21°S) (Novello *et al.*, 2017); C) δO^{18} speleothem records from Lapa Grande (14°S)/Lapa Sem Fim (16°S) (Stríkis *et al.*, 2011; 2015); D) δO^{18} speleothem records from Botuverá (27°S) (Cruz *et al.*, 2005; Wang *et al.*, 2007); E) PC1 scores curve representing vegetation trends in central Cerrados, along with climatic significance and charcoal influx for Lagoa Feia (LF) and São José (SJ). δO^{18} data are available at the SISAL database (Atsawawaranunt *et al.*, 2019). *The age limits of the global Youger Dryas (YD) event (beige background) are based on Broecker *et al.* (2010).

During the early-middle Holocene (~11,000 to 7,000 cal yr BP), the PC1 curve reflecting vegetation variability in the Central Cerrados demonstrates relatively dry conditions at Lagoa Feia and São José, anti-phased with wetter/colder conditions at Salitre. The Lagoa Feia record indicates that this early-middle Holocene dryness in northern central Cerrados was related to the repeated occurrence of dry events, interspersed with wetter events, during a period of weakened SASM activity. This agrees with the abrupt centennial-scale variations in precipitation detected on the Lapa Grande/Lapa Sem Fim and Jaraguá δO^{18} records during the Holocene (Stríkis *et al*., 2011; Novello *et al*., 2017). The δO^{18} record from Botuverá, in southern Brazil, also showed drier conditions during this period, and these conditions could also be attributed to weaker SASM (Fig. 8). Wet and dry episodes are not synchronous in the δO^{18} records, which may reflect repeated shifts in the southern boundary belt of the SASM during the early Holocene along with effects from northward polar advection. For instance, a dry event centered around 7,800 cal yr BP in Lapa Grande (Stríkis *et al*., 2011) coincides with a wet event in the Botuverá record, suggesting a southward displacement of the SASM belt at that time.

The interplay between these repeated shifts in the southern boundary belt of the SASM with the northward polar advection could explain the anti-phase between São José/Lagoa Feia and Salitre. Weaker SASM activity would have allowed frequent and intense polar mass activity at Salitre (Fig. 9), resulting in the development of a moist forest including a mixture of tropical and cold-adapted taxa (Ledru, 1993). Polar air masses have two dominant northward trajectories in southern Brazil: one follows the Atlantic coast and the other penetrates the continent through the Paraná River valley (Boin, 2005). Modern observations have shown that years characterized by weakened tropical Atlantic air mass activity offer less resistance to polar fronts. Hence, during these years the polar fronts can penetrate deep into the Paraná River valley, causing climatic instability and rains in southern and southeastern Brazil (Boin, 2005). Although Salitre is located only 300 and 400 km from São José and Lagoa Feia, respectively, the current vegetation (savanna at Lagoa Feia and São José, and Atlantic semi-deciduous forest at Salitre) shows that the higher altitude and topographic setting of Salitre, located in the highlands bordering the upper Paraná River, cause it to be more affected by polar mass activity. In fact, as the air masses move northward through the Paraná valley they are blocked by the highlands at the upper portion of the valley. As a result, winter rains frequently occur in this area, but the precipitation does not reach the more central regions of the Brazilian highlands where São José and Lagoa Feia are located (Vera et al 2006).

The occurrence of sedimentary or pollen hiatuses during the Pleistocene-Holocene transition and early Holocene in the other two previously studied pollen records in Central Cerrados, namely, Cromínia (Salgado-Labouriau *et al*., 1997a) and Águas Emendadas (Barberi *et al*., 2000), is likely a consequence of the dry conditions during the early Holocene. Both of these records (Cromínia and Águas Emendadas) were collected from palm swamps, which are shallow depositional sites that are more vulnerable to total drying and erosion than sites like Lagoa Feia. A lake environment was present at the Lagoa Feia site throughout the early Holocene, although it was prone to seasonal temporary dryness. The presence of early Holocene sediments with preserved pollen in the Lagoa Feia record proves that a total desertification of the central Cerrados did not occur in the Holocene period, and that arboreal savanna was part of the landscape even during drier phases. The continuity of a moist depositional environment during the early Holocene at Lagoa Feia has also allowed the preservation of older sediments and provided insight into time periods for which data could not be obtained from other Cerrados sites, i.e., the Younger Dryas wet event. Therefore, the aridification trend that was previously presented for the central Cerrados based on paleoecological records actually corresponds to shifts between dry and wet episodes during the early Holocene (Fig. 9).

Between ~6,500-5,200 cal yr BP, central Cerrados pollen records show a trend towards relatively wet conditions, e.g., expansion of the São José palm swamp, increasing lake levels at Lagoa Feia, and a re-expansion of the palm swamps at Cromínia (Salgado-Labouriau *et al*., 1997a) and Águas Emendadas (Barberi *et al*., 2000). These data indicate that moisture supply from SASM activity became more regular than it had been during the early Holocene, although the climate at this time period was still relatively drier than it is currently (Prado *et al*., 2013). A reconstruction of local moisture from the $^{87}Sr/^{86}Sr$ speleothem record of Tamboril cave, located around 60 km south of Lagoa Feia in central Brazil, disagrees with this trend, as the record indicated drier conditions from around 6,000 to 2,000 cal yr BP relative to a wetter early Holocene (Ward *et al*., 2019). However, this finding might reflect different local conditions of the Tamboril cave, as most sites in central Brazil show a trend of increasing humidity from the middle Holocene onwards. This trend also coincides with wetter conditions in the Botuverá δO^{18} record from southern Brazil, and can be linked to stronger SASM activity and increasing summer insolation in the SH from the middle Holocene to the present (Cruz *et al*., 2005; Ward *et al*., 2019). The Lapa Grande/Lapa Sem Fim δO^{18} record is not continuous in the middle Holocene, but showed a strong wet event

centered at around 5,200 cal yr BP (Stríkis *et al.*, 2011). Increasing SASM activity in southern and central Brazil from the middle Holocene onwards is correlated with increasing dryness in northern South America (Haug *et al.*, 2001) and northeastern Brazil (De Oliveira *et al.*, 1999; Cruz *et al.*, 2009) starting around 6,000 - 5,000 cal yr BP. This trend reflects the interplay between the southward displacement of the ITCZ, increased convection in central South America and enhanced subsidence in northeastern Brazil.

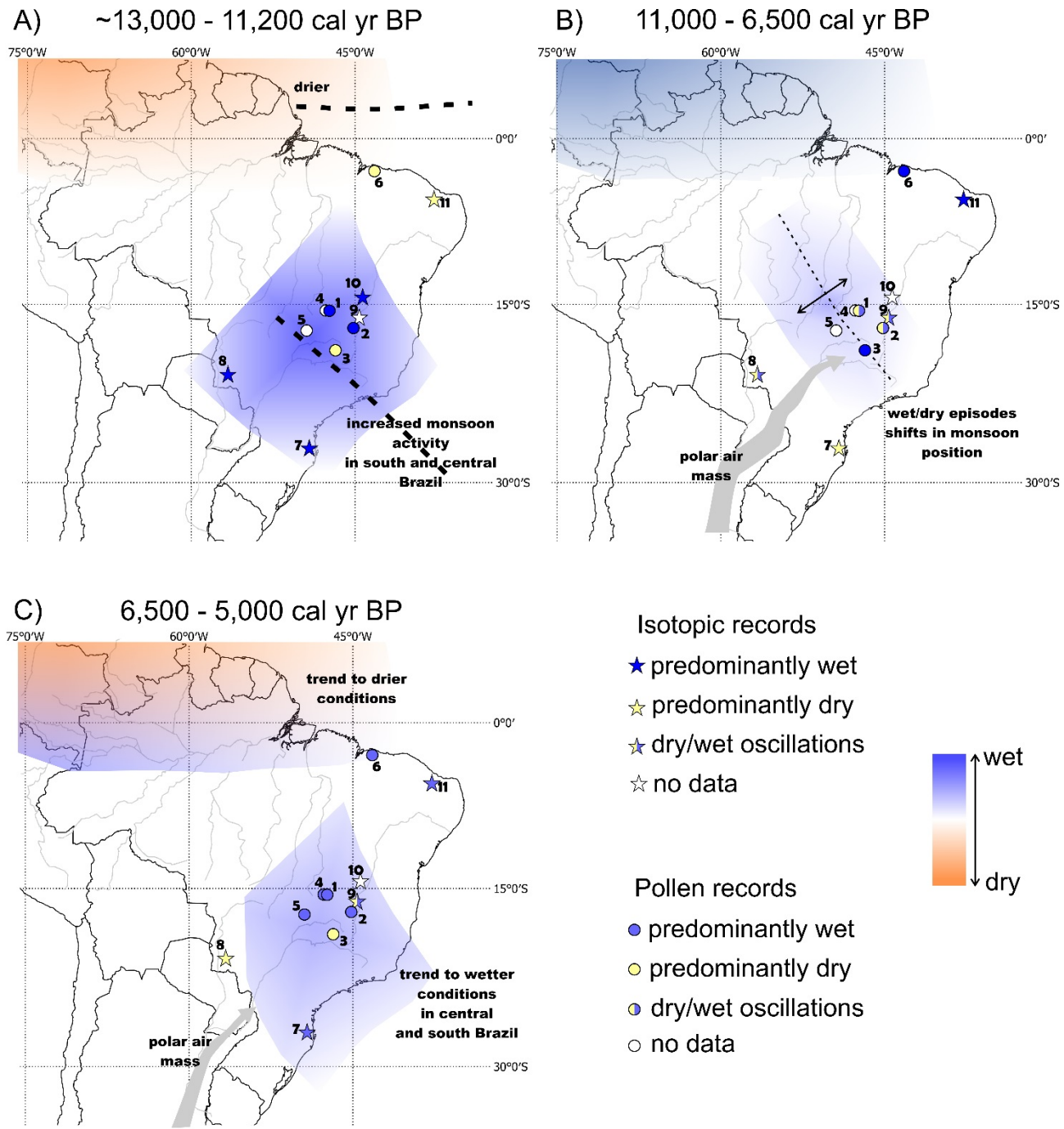


Figure 9: Schematic representation of SASM position and activity during the Pleistocene-Holocene transition and early-middle Holocene in central Cerrados. A) ~13,000 to 11,200 cal yr BP; B) 11,000 to 6,500 cl yr BP; C) 6,500 to 5,000 cal yr BP. Pollen sites: 1. Lagoa Feia (this study); 2. São José (Cassino *et al.*, 2018); 3. Salitre (Ledru, 1993; Ledru *et al.*, 1996);

4. Águas Emendadas (Barberi *et al*., 2000); 5. Cromínia (Salgado-Labouriau *et al*., 1997a); 6. Caçó (Ledru *et al*., 2006). Speleothem records: 7. Botuverá (Cruz *et al*., 2005; Wang *et al*., 2007) ; 8. Jaraguá (Novello *et al*., 2017) ; 9. Lapa Grande (Strikís *et al*., 2011 ; Stríkis *et al*., 2015); 10. Lapa Sem Fim (Stríkis *et al*., 2015); 11. Rio Grande do Norte (Cruz *et al*., 2009). Trends for northern South America are based on research from Haug *et al*., 2001 and Maslin *et al*., 2011.

Similar trends in charcoal influx between the Lagoa Feia and São José sites suggest a link between fire activity and SASM variability. During the wet Younger Dryas, charcoal was not abundant in the Lagoa Feia and São José records, with the exception of one peak of large charcoal particles in the São José record that could be related to a single local fire. Fire activity increased at both sites around 10,800 cal yr BP following the onset of drier conditions during the early Holocene. The decreased SASM activity in central Brazil and the subsequent longer, more severe dry season, along with the high fuel availability inherited from the previous wet period, is likely to have triggered this increase in fire activity. The intense fire activity corresponded to a decrease in arboreal cover at Lagoa Feia, which suggests that fire plays an important role in vegetation turnover across the central Cerrados. This contrasts with results obtained from Laguna La Gaiba (Power *et al*., 2016), which lies in the transition between seasonally dry tropical forests and Pantanal on the border between Bolivia and Brazil. The Laguna La Gaiba record also suggests a drier early-middle Holocene, but with a different timing compared to the central Cerrados: dryness appeared between 10,000-4,000 cal yr BP and was related to changes in forest composition. However, the charcoal record from Laguna La Gaiba shows an intensification of fire activity around 7,500 cal yr BP, approximately two millennia after the onset of drier conditions, and this intensification of fire was not correlated with a change in vegetation. Hence, data from Laguna La Gaiba suggest that fire had a limited influence on vegetation at that site (Power *et al*., 2016), which contrasts with our results for the Cerrados.

6. Conclusions

The Pleistocene-Holocene transition and early Holocene are characterized by a succession of wet and dry episodes related to shifts in the SASM boundary belt. These shifts in rainfall distribution affected biodiversity, vegetation structure and fire activity in the central Cerrados.

During the last 13 kyr, three main phases were identified from pollen records from central Brazil. The first phase, between 13,000 and 11,200 cal yr BP, showed noticeably increased SASM activity in central Brazil, which was linked to a forested landscape and low fire activity. This finding agreed with speleothem records from latitudes between 15° to 27°S. The next phase, which occurred during the early-middle Holocene, was characterized by centennial-scale oscillations between dry and wet episodes, which caused alternating expansion

and regression phases of arboreal cover and lake levels at Lagoa Feia. The SASM belt shifted significantly, and multiple times, in the central Cerrados between 11,200 and 6,500 cal yr BP, and the presented findings suggest that these oscillations intensified the influence of polar air masses in the interior of southeastern Brazil. Fire activity increased for a short period right after 11,000 cal yr BP in the central Cerrados, which coincided with the identified decrease in arboreal cover, and then decreased during most of the early Holocene. During the final distinct phase, between ~ 6,500 and 5,000 cal yr BP, climate conditions in the central Cerrados were relatively wetter than what had been witnessed during the early Holocene, but drier than modern conditions.

Acknowledgements

This work was supported by UMR ISEM and IRD and is part of the projects - Dimensions of biodiversity FAPESP (BIOTA 444 2013/50297-0), NSF (DEB 1343578) and NASA, and the Labex-CEBA. We thank Anne-Lise Develle at the Laboratoire Environnement Dynamique Territoire Montagne (EDYTEM) (University of Savoie, CNRS) for her assistance in the XRF scanning analyses, Vania Pivello (Ib-USP) for her assistance in the fieldwork, Boromir Bogumil for filming the fieldwork at Lagoa Feia (film available at: https://www.youtube.com/watch?v=sz3zV7QC_H0), and Paulo de Oliveira (USP) for lending us the corer and boats used to core at Lagoa Feia.

Bibliography

Alvares, C.A., Stape, J.L., Sentelhas, P.C., Gonçalves, J.L.M., Sparovek, G. 2013. Köppen's climate classification map for Brazil. *Meteorologische Zeitschrift*. 22(6), 711-728. doi:10.1127/0941-2948/2013/0507

Assis, A.C., Coelho, R.M., Pinheiro, E.S., Durigan, G. 2010. Water availability determines physiognomic gradient in an area of low-fertility soils under Cerrado vegetation. *Plant Ecology*. 212, 1135-1147. DOI 10.1007/s11258-010-9893-8

Atsawawaranunt, K., Harrison, S., Comas-Bru, L. 2019. SISAL (Speleothem Isotopes Synthesis and AnaLysis Working Group) database version 1b. Dataset. University of Reading, Reading, United Kingdom. http://dx.doi.org/10.17864/1947.189

Barberi, M., Salgado-Labouriau, M.L., Suguio, K. 2000. Paleovegetation and paleoclimate of "Vereda de Águas Emendadas'', central Brazil. *Journal of South American Earth Sciences*. 13, 41-254. https://doi.org/10.1016/S0895-9811(00)00022-5.

Bennett, K.D., Willis, K.J. 2001. Pollen. *In:* Smol, J.P., Birks, H.J.B., Last, W.M. (Eds.) *Tracking Environmental Change Using Lake Sediments*, Vol. 3, Terrestrial, Algal, and Siliceous Indicators. Kluwer Academic Publishers, Dordrecht, Netherlands, p. 5-32.

Blaauw, M., Christen, J.A. 2011. Flexible paleoclimate age-depth models using an autoregressive gamma process. *Bayesian Analysis*. 6(3), 457-474. DOI:10.1214/11-BA618

Boin, M.N., Zavattini, J.A. 2005. Variações do ritmo pluvial no oeste paulista: gênese e impactos erosivos. *Geografia*. 30(1), 115-139.

Broecker, W.S., Denton, G.H., Edwards, R.L., Cheng, H., Alley, R.B., Putnam, A.E. 2010. Putting the Younger Dryas cold event into context. *Quaternary Science Reviews*. 29(9-10), 1078-1081. https://doi.org/10.1016/j.quascirev.2010.02.019.

Cabral, O.M.R., Da Rocha, H.R., Gash, J.H., Freitas, H.C., Ligo, M.A.V. 2015. Water and energy fluxes from a woodland savanna (cerrado) in southeast Brazil. *Journal of Hydrology: Regional Studies*. 4, 22-40, https://doi.org/10.1016/j.ejrh.2015.04.010.

Cassino, R.F., Martinho, C.T., Caminha, S.A.F.S. 2018. A Late Quaternary palynological record of a palm swamp in the Cerrado of central Brazil interpreted using modern analog data. *Palaeogeography, Palaeoclimatology, Palaeoecology*. 490, 1-16. 10.1016/j.palaeo.2017.08.036.

Cheng, H., Fleitmann, D., Edwards, L.R., Wang, X., Cruz, F.W., Auler, A.S., Mangini, A., Wang, Y., Kong, X., Burns, S.J., Matter, A. 2009. Timing and structure of the 8.2 kyr B.P. event inferred from δ18O records of stalagmites from China, Oman, and Brazil. *Geology*. 37, 1007-1010. doi:10.1130/G30126A.1.

Cheng, H., Sinha, A., Cruz, F.W.J., Wang, X., Edwards, R.L., D'horta, F.M., Ribas, C.C., Vuille, M., Stott, L.D., Auler, A.S. 2013. Climate change patterns in Amazonia and biodiversity. *Nature Communications*. 4, 1-6. doi:10.1038/ncomms2415

Cruz, F.W.J., Burns, S.J., Karmann, I., Sharp, W.D., Vuille, M., Cardoso, A.O., Ferrari, J.A., Silva Dias, P.L., Viana, O. 2005. Insolation-driven changes in atmospheric circulation over the past 116,000 years in subtropical Brazil. *Nature*. 434(7029), 63-66. doi:10.1038/nature03365

Davies, S.J., Lamb, H.F., Roberts, S.J. 2015. Micro-XRF core scanning in palaeolimnology: recent developments. *In*: Croudace, I.W., Rothwell, R.G. (Eds.) *Micro-XRF studies of sediment cores: Applications of a non-destructive tool for the environmental sciences*. Developments in Paleoenvironmental Research, 17, Springer, Dordrecht, Netherlands, p. 189-226. DOI 10.1007/978-94-017-9849-5_7

De Oliveira, A.L.R., Gil, A.S.B, Bove, C.P. 2011. Hydrophytic Cyperaceae from the Araguaia river basin, Brazil. *Rodriguésia*. 62(4), 847-866. http://dx.doi.org/10.1590/S2175-78602011000400012

De Oliveira, P.E., Barreto A.M.F., Suguio K. 1999. Late Pleistocene/Holocene climatic and vegetational history of the Brazilian Caatinga: the fossil dunes of the middle São Francisco River. *Paleogeography, Paleoclimatology, Paleoecology.* 152, 319-337. https://doi.org/10.1016/S0031-0182(99)00061-9

Durigan, G., Ratter, J.A. 2016. The need for a consistent fire policy for Cerrado conservation. *Journal of Applied Ecology.* 53, 11-15. https://doi.org/10.1111/1365-2664.12559

Fank-De-Carvalho, S.M., Marchioretto, M.S., Báo, S.N. 2010. Anatomia foliar, morfologia e aspectos ecológicos das espécies da família Amaranthaceae da Reserva Particular do Patrimônio Natural Cara Preta, em Alto Paraíso, GO, Brasil. *Biota Neotropica.* 10, 77-86. http://dx.doi.org/10.1590/S1676-06032010000400011.

Fank-De-Carvalho, S.M., Somavilla, N.S., Marchioretto, M.S., Báo, S.N. 2015. Plant Structure in the Brazilian Neotropical Savannah Species. *In:* Lo, Y-H., Blanco, J.A., Roy, S. (Eds.) *Biodiversity in Ecosystems - Linking Structure and Function*. InTech, London, United Kingdom, p. 407-442. DOI: 10.5772/59066.

Ferraz-Vicentini, K. 1999. *História do fogo no Cerrado: uma análise palinológica.* Unpublished PhD Thesis. Departamento de Ecologia, Universidade de Brasília, Brasília, Brazil.

Fick, S.E., Hijmanns, R.J. 2017. Worldclim 2: New 1-km spatial resolution climate surfaces for global land areas. *International Journal of Climatology*. 37, 4302-4315. https://doi.org/10.1002/joc.5086

Fiedler, N.C., Merlo, D.A., Medeiros, M.B. 2006. Ocorrência de incêndios florestais no Parque Nacional da Chapada dos Veadeiros. *Ciência Florestal*. 16, 153-161. http://dx.doi.org/10.5902/198050981896

Furley, P.A. 1999. The nature and diversity of neotropical savanna vegetation with particular reference to the Brazilian Cerrados. *Global Ecology and Biogeography*. 8, 223-241. https://doi.org/10.1046/j.1466-822X.1999.00142.x

Gosling, W., Mayle, F.E., Tate, N.J., Killeen, T.J. 2009. Differentiation between Neotropical rainforest, dry forest, and savannah ecosystems by their modern pollen spectra and implications for the fossil pollen record. *Review of Palaeobotany and Palynology*. 153, 70-85. 10.1016/j.revpalbo.2008.06.007

Haug, G.H., Hughen, K.A., Sigman, D.M., Peterson, L.C., Röhl, U. 2001. Southward Migration of the Intertropical Convergence Zone through the Holocene. *Science*. 293(5533), 1304-1308. DOI: 10.1126/science.1059725

Hoffmann, W.A., Moreira, A.G. 2002. The Role Of Fire In Population Dynamics Of Woody. *In*: Oliveira, P.S., Marquis, R.J. (Eds.). *The cerrados of Brazil: ecology and natural history of a neotropical savanna*. Columbia University Press, New York, p. 159-177. DOI: 10.7312/oliv12042

Hogg, A., Hua, Q., Blackwell, P., Niu, M., Buck, C., Guilderson, T., Heaton, T., Palmer, J., Reimer, P., Reimer, R., Turney, C., Zimmerman, S. 2013. SHCal13 Southern Hemisphere Calibration, 0–50,000 Years cal BP. *Radiocarbon*. 55(4), 1889-1903. DOI: 10.2458/azu_js_rc.55.16783

IBGE. 2002. Climate map of Brazil, scale 1:500000, Instituto Brasileiro de Geografia e Estatística, Rio de Janeiro, Brazil.

IBGE. 2004. Map of Brazilian biomes, scale 1:500000, Instituto Brasileiro de Geografia e Estatística, Rio de Janeiro, Brazil.

Juggins, S. 2007. C2 Version 1.5 User guide. Software for ecological and palaeoecological data analysis and visualisation. Newcastle University, Newcastle upon Tyne, United Kingdom, 73pp.

Klink, C.A., Moreira, A.G. 2002. Past and current human occupation, and land use. *In*: Oliveira, P.S., Marquis, R.J. (Ed.). *The Cerrados of Brazil: Ecology and Natural History of a Neotropical Savanna*. Columbia University Press, New York, p. 69-88. DOI: 10.7312/oliv12042

Kutzbach, J.E, Liu, X., Liu, Z., Chen, G. 2008. Simulation of the evolutionary response of global summer monsoons to orbital forcing over the past 280,000 years. *Climate Dynamics*. 30, 567-579. doi: 10.1007/s00382-007-0308-z

Lacerda Filho, J.V., Rezende, A., Da Silva, A. (Ed.) 2000. Programa Levantamentos Geológicos Básicos do Brasil. Geologia e Recursos Minerais do Estado de Goiás e do Distrito Federal, Scale 1:500.000, CPRM, Goiânia, Brazil.

Lea, D.W., Pak, D.K., Peterson, L.C., Hughen, K.A. 2003. Synchroneity of Tropical and High-Latitude Atlantic Temperatures over the Last Glacial Termination. *Science*. 301, 1361-1364 DOI: 10.1126/science.1088470

Ledru, M.-P. 1993. Late Quaternary Environmental and Climatic Changes in Central Brazil. *Quaternary Research*. 39(1), 90-98. https://doi.org/10.1006/qres.1993.1011

Ledru, M.-P., Braga, P.I.S., Soubiès, F., Fournier, M., Martin, L., Suguio, K., Turcq, B. 1996. The last 50,000 years in the Neotropics (Southern Brazil): evolution of vegetation and climate. *Palaeogeography, Palaeoclimatology, Palaeoecology*. 123, 239-257. https://doi.org/10.1016/0031-0182(96)00105-8

Ledru, M.-P., Ceccantini, G., Gouveia, S.E.M., López-Sáez, J.A., Pessenda, L.C.R., Ribeiro, A.S. 2006. Millenial-scale climatic and vegetation changes in a northern Cerrado (Northeast, Brazil) since the Last Glacial Maximum. *Quaternary Science Reviews*. 25, 1110-1126. doi:10.1016/j.quascirev.2005.10.005

Marchant, R., Almieda, L., Behling, H., Berrio, J. C., Bush, M., Cleef, A., Duivenvoorden, J., Kappelle, M., De Oliveira, P., Teixeira De Oliveira Filho, A., Garcia-Lozano, S., Hooghiemstra, H., Ledru, M.-P., Markgraf, V., Mancici, V., Paez, M., Prieto, A., Salgado-Labouriau, M.L. 2002. Distribution and ecology of parent taxa of

pollen lodged within the Latin American Pollen Database. *Review of Palaeobotany and Palynology*. 121, 1-75. https://doi.org/10.1016/S0034-6667(02)00082-9

Maslin, M.A., Ettwein, V.J., Wilson, K.E., Guilderson, T. P., Burns, S.J., Leng, M.J. 2011. Dynamic boundary-monsoon intensity hypothesis: evidence from the deglacial Amazon River discharge record. *Quaternary Science Reviews*. 30, 3823-3833. https://doi.org/10.1016/j.quascirev.2011.10.007

Medeiros, M.B., Fiedler, N.C. 2004. Incêndios florestais no Parque Nacional da Serra da Canastra: desafios para a conservação da biodiversidade. *Ciência Florestal*. 14, 157-168. http://dx.doi.org/10.5902/198050981815

Medina, C.L., Sanches, M.C., Tucci, M.L.S., Sousa, C.A.F., Rogério, G., Cuzzuol, F., Joly, C.A. 2009. *Erythrina speciosa* (Leguminosae-Papilionoideae) under soil water saturation: morphophysiological and growth responses. *Annals of Botany*. 104, 671–680. doi:10.1093/aob/mcp159.

Mendonça, R.C., Felfili, J.M., Walter, B.M.T., Silva Júnior, M.C., Rezende, A.V., Figueira, J.S., Nogueira, P.E. 2008. Flora vascular do bioma Cerrado: um "checklist" com 11.430 espécies. *In:* Sano, S.M., Almeida, S.P., Ribeiro, J.F. (Eds.) *Cerrado: Ecologia e Flora.* v.2. Embrapa Informação Tecnológica, Brasília, p. 423-1279.

Miranda, H.S., Neto, W.N., Neves, B.M.C. 2010. Caracterização das queimadas de Cerrado. *In:* Miranda, H.S. (Ed.) *Efeitos do regime de fogo sobre a estrutura de comunidades de Cerrado: Projeto Fogo*, Ed. Ibama, Brasília, Brazil, p. 23-35. ISBN 978-85-7300-305-5

Mistry, J. 1998. Fire in the cerrado (savannas) of Brazil: an ecological review. *Progress in Physical Geography.* 22(4), 425-448. https://doi.org/10.1177/030913339802200401

Moreira, A.G. 2000. Effects of fire protection on savanna structure in Central Brazil. *Journal of Biogeography*. 27, 1021-1029. https://doi.org/10.1046/j.1365-2699.2000.00422.x

Motta, P.E.F., Curi, N., Franzmeier, D.P. 2002. Relation of Soils and Geomorphic Surfaces in the Brazilian Cerrado *In*: OLIVEIRA P.S., MARQUIS R.J. (Eds.). *The cerrados of Brazil: ecology and natural history of a neotropical savanna*. Columbia University Press, New York, p. 33-50. DOI: 10.7312/oliv12042

Novello, V.F., Cruz Júnior, F.W., Vuille, M., Karmann, I., Santos, R.V., Strikis, N.M., Wang, X., Emerick, S., Paula, M.S.De, Xianglei, L., Hai, C., Edwards, R.L., Barreto, E.D.E.S. 2017. A high-resolution history of the South American monsoon from last glacial maximum to the Holocene. *Scientific Reports*. 7, 44267. doi:10.1038/srep44267

Oliveira-Filho, A.T., Ratter, J.A. 2002. Vegetation physiognomies and woody flora of the Cerrado biome. *In*: Oliveira, P.S., Marquis, R.J. (Eds.). *The cerrados of Brazil: ecology and natural history of a neotropical savanna*. Columbia University Press, New York, p. 91-120. DOI: 10.7312/oliv12042

Oliveras, I., Meirelles, S.T., Hirakuri, V.L., Freitas, C.R., Miranda, H.S., Pivello, V.R. 2013. Effects of fire regimes on herbaceous biomass and nutrient dynamics in the Brazilian savanna. *International Journal of Wildland Fire*. 22, 368-380. https://doi.org/10.1071/WF10136

Power, M.J., Whitney, B.S., Mayle, F.E., Neves, D.M., De Boer, E.J., Maclean, K.S. 2016. Fire, climate and vegetation linkages in the Bolivian Chiquitano seasonally dry tropical forest. *Philosophical Transactions of the Royal Society B Biological Sciences*. 371, 165. http://dx.doi.org/10.1098/rstb.2015.0165

Prado, L.F., Wainer, I., Chiessi, C.M., Ledru, M.-P., Turcq, B. 2013. A mid-Holocene climate reconstruction for eastern South America. *Climate of the Past*. 9, 2117-2133. https://doi.org/10.5194/cp-9-2117-2013

Project MapBiomas - Collection 2 of Brazilian Land Cover & Use Map Series, accessed on April, 2019 through the link: https://mapbiomas.org/en.

Ramos-Neto, M.B., Pivello, V.R. 2000. Lightning Fires in a Brazilian Savanna National Park: Rethinking Management Strategies. *Environmental Management*. 26(6), 675-684. DOI: 10.1007/s002670010124

Ratter, J.A., Bridgewater S., Atkinson R., Ribeiro J. F. 1996. Analysis of the floristic composition of the Brazilian cerrado vegetation II: comparison of the woody vegetation of 98 areas. *Edinburgh Journal of Botany*. 53, 153-180. DOI: https://doi.org/10.1017/S0960428600002821

Ribeiro, J.F., Walter, B.M.T. 2008. As principais fitofisionomias do Cerrado. *In*: SANO S.M., ALMEIDA S.P., RIBEIRO J.F. (Eds.), *Cerrado: Ecologia e Flora*, vol.1. Embrapa Informação Tecnológica, Brasília, Brazil, p. 151-199.

Rojas, M., Arias, P. A., Flores-Aqueveque, V., Seth, A., Vuille, M. 2016. The South American monsoon variability over the last millennium in climate models. *Climate of the Past*. 12, 1681–1691. https://doi.org/10.5194/cp-12-1681-2016

Salgado-Labouriau, M.L., Casseti, V., Ferraz-Vicentini, K.R., Martin, L., Soubiés, F., Suguio, K., Turcq, B. 1997. Late Quaternary vegetational and climatic changes in cerrado and palm swamp from Central Brazil. *Palaeogeography, Palaeoclimatology, Palaeoecology*. 128, 215-226. https://doi.org/10.1016/S0031-0182(96)00018-1

Sato, M.N., Miranda, H.S., Maia, J.M.F. 2010. O fogo e o estrato arbóreo do Cerrado: efeitos imediatos e de longo prazo. *In:* Miranda, H.S. (Ed.) *Efeitos do regime de fogo sobre a estrutura de comunidades de Cerrado: Projeto Fogo*, Ed. Ibama, Brasília, Brazil, p.78-92. ISBN 978-85-7300-305-5

Schneider, T., Bischoff, T., Haug, G.H. 2014. Migrations and dynamics of the intertropical convergence zone. *Nature*. 513(7516), 45-53. doi: 10.1038/nature13636.

Silva, F.A.M., Assad, E.D., Steinke, E.T., Muller, A.G. 2008. O Clima do Bioma Cerrado. *In:* Albuquerque, A.C.S., Da Silva, A.G. (Eds). *Agricultura Tropical: Quatro décadas de inovações tecnológicas, institucionais e políticas*. Embrapa Informações Tecnológicas, Brasília, Brazil, p. 93-148. ISBN: 978-85-7383-432-1

Silva, V.B.S., Kousky, V.E. 2012. The South American Monsoon System: Climatology and Variability. In: Wang, S-Y., Gillies, R.R. (Eds). *Modern climatology*. InTech, London, United Kingdom, p. 123-152. DOI: 10.5772/38565.

Simon, M.F., Grether, R., De Queiroz, L.P., Skema, C., Pennington, R.T, Hughes, C.E. 2009. Recent assembly of the Cerrado, a neotropical plant diversity hotspot, by in situ evolution of adaptations to fire. *Proceedings of the National Academy of Sciences*. 106(48), 20359–20364. https://doi.org/10.1073/pnas.0903410106

Stockmarr, J. 1971. Tablets with spores used in absolute pollen analysis. *Pollen Spores*. 13, 615-621.

Stríkis, N.M., Chiessi, C.M., Cruz, F.W., Vuille, M., Cheng, H., Barreto, E.A.S., Mollenhauer, G., Kasten, S., Karmann, I., Edwards, R.L., Bernal, J.P., Sales, H.D.R. 2015. Timing and structure of Mega-SACZ events during Heinrich Stadial 1. *Geophysical Research Letters*. 42, 1-8. https://doi.org/10.1002/2015GL064048

Stríkis, N.M., Cruz, F.W., Cheng, H., Karmann, I., Edwards, R.L., Vuille, M., Wang, X., De Paula, M.S. Novello, V.F. 2011. Abrupt Variations in South American Monsoon Rainfall during the Holocene based on a Speleothem Record from Central-Eastern Brazil. *Geology*. 39(11), 1075-1078.

Stríkis, N.M., Cruz Júnior, F.W., Barrteto, E.A.S., Naughton, F., Vuille, M., Cheng, H., Voelker, A.H.L., Zhang, H., Karmann, I., Edwards, R.L., Auler, A.S., Santos, R.V., Sales, H.R. 2018. South American monsoon response to iceberg discharge in the North Atlantic. *Proceedings of the National Academy of Sciences*. 115, 3788-3793. doi:10.1073/pnas.1717784115

Terra, M.C.N.S., Dos Santos, R.M., Prado Júnior, J.P., De Mello, J.M., Scolforo, J.R.C., Fontes, M.A.L.F., Schiavini, I., Dos Reis, A.A., Bueno, I.T., Magnago, L.F.S., Ter Steege, H. 2018. Water availability drives gradients of tree diversity, structure and functional traits in the Atlantic–Cerrado–Caatinga transition, Brazil. *Journal of Plant Ecology*. 11(6), 803-814. doi: 10.1093/jpe/rty017

Vera, C., Higgins, W., Amador, J., Ambrizzi, T., Garreaud, R., Gochis, D., Gutzler, D., Lettenmaier, D., Marengo, J., Mechoso, C.R., Nogues-Paegle, J., Silva Dias, P.L., Zhang, C. 2006. Toward a unified view of the American Monsoon Systems. *Journal of Climate*. 19, 4977-5000. doi:10.1175/JCLI3896.1

Walker, M., Head, M.J., Berkelhammer, M., Björck, S., Cheng, H., Cwynar, L., Fisher, D., Gkinis, V., Long, A., Lowe, J., Newnham, R., Rasmussen, S.O., Weiss, H. 2018. Formal ratification of the subdivision of the Holocene Series/Epoch (Quaternary System/Period), two new Global Boundary Stratotype Sections and Points (GSSPs) and three new stages/subseries. *Episodes*. 41, 213-223. https://doi.org/10.18814/epiiugs/2018/018016

Wang, X., Edwards, R. L., Auler, A. S., Cheng, H., Ito, E. 2007. Millennial-scale interhemispheric asymmetry of low-latitude precipitation: speleothem evidence and possible high-latitude forcing. In: Schmittner, A., Chiang, J.C., Hemming, S.R. (Eds). *Ocean Circulation: Mechanisms and Impacts - Past and Future Changes of Meridional Overturning*, *Geophysical Monograph Series*, American Geophysical Union, Washington, D.C., 173, 279-294. doi:10.1029/173GM18

Wang, X., Edwards, R., Auler, A., Cheng, H., Kong, X., Wang, Y., Cruz, F.W., Dorale, J.A., Chiang, H.W. 2017. Hydroclimate changes across the Amazon lowlands over the past 45,000 years. *Nature*. 541, 204-207. https://doi.org/10.1038/nature20787

Ward, B.M., Wong, C.I., Novello, V.F., Mcgee, D., Santos, R.V., Silva, L.C.R., Cruz, F.W., Wang, X., Edwards, R.L., Cheng, H. 2019. Reconstruction of Holocene coupling between the South American Monsoon System and local moisture variability from speleothem $\delta^{18}O$ and $^{87}Sr/^{86}Sr$ records. *Quaternary Science Reviews*. 210, 51-63. https://doi.org/10.1016/j.quascirev.2019.02.019

Willard, D., Bernhardt, C.E., Weimer, L.G., Cooper, S.R., Gámez, D., Jensen, J.A. 2004. Atlas of pollen and spores of the Florida Everglades. *Palynology*. 28, 175–227. doi/abs/10.1080/01916122.2004.9989597

List of tables

Table 01: Radiocarbon dates of the LF15-2 core.

List of figures

Figure 01: Geographic distribution and climate of the Cerrados, locations from which pollen and isotopic records mentioned in this study were collected, and geology and vegetation of the Lagoa Feia site..

Figure 02: Lithology and age-depth model for the LF15-2 sediment core.

Figure 03: XRF scanning results showing the levels of selected elements (Zr, Si, Rb, K, Al, Fe, Zn, Ti, Ca, Sr, S), along with relevant ratios (Rb/K, Fe/Ti, Zn/Ti, Si/Ti, Ca/Ti, S/Ti), for core LF15-2 plotted against depth.

Figure 04: Synthetic pollen percentage diagram for the LF15-2 core, with data plotted against depth (y-axis).

Figure 05: Summary pollen diagram for the LF15-2 core, with the data plotted against time (cal yr BP).

Figure 06: Synthetic representation of paleoecological changes over the last 16,000 years observed from the Lagoa Feia (this study), São José and Salitre cores (from Cassino et al., 2018 and Ledru, 1993, respectively).

Figure 07: Principal Components Analysis of interpolated pollen data from Lagoa Feia, São José and Salitre records.

Figure 08: Comparison of vegetation cover variability in central Cerrados and δO18 speleothem records from adjacent regions.

Figure 09: Schematic representation of SASM position and activity during the Pleistocene-Holocene transition and early-middle Holocene in central Cerrados.

859

75
76

Supplementary Material

Table 1: List of pollen taxa identified from the Lagoa Feia core

Pollen taxa	Family	Habitat (Cerrados physiognomy)[1]	Life-form type[1, 2]
Acacia-Type	Fabaceae	forest, savanna, dry forest	tree, bindweed
Acalypha cf. diversifolia	Euphorbiaceae	forest	shrub
Acalypha sp.	Euphorbiaceae	grassland, forest	shrub, herb
Acosmium-Type	Fabaceae	savanna, dry forest, forest, grassland	tree, shrub
Alchornea sp.	Euphorbiaceae	forest	tree
Alternanthera sp.	Amaranthaceae	grassland, savanna, forest, swamp	herb, subshrub
Amaranthus-Type	Amaranthaceae	-	herb
Anadenanthera-Type	Fabaceae	forest, dry forest	tree
Andira-Type	Fabaceae	forest, dry forest, savanna	tree, shrub
Annonaceae	Annonaceae	savanna, dry forest, forest, grassland, swamp	tree, shrub, subshrub
Aphelandra sp.	Acanthaceae	-	shrub, herb, subshrub
Apuleia leiocarpa	Fabaceae	forest	tree
Asteraceae	Asteraceae	grassland, savanna, dry forest, forest, swamp, palm swamp	all
Astronium-Type	Anacardiaceae	savanna, forest	tree
Attalea-Type	Arecaceae	savanna, forest	shrub, tree
Banisteriopsis-Type	Malpighiaceae	savanna, forest, grassland	shrub, bindweed, subshrub, tree
Bauhinia sp.	Fabaceae	forest, savanna, grassland, dry forest	shrub, subshrub, bindweed
Begonia sp.	Begoniaceae	forest, grassland	herb
Borreria-Type	Rubiaceae	savanna, grassland	herb, subshrub, shrub
Brosimum-Type	Moraceae	savanna, grassland, forest	shrub, tree
Byrsonima sp.	Malpighiaceae	savanna, forest, grassland, swamp, palm swamp, dry forest	tree, shrub, subshrub, herb,
Cactaceae	Cactaceae	savanna, forest	herb, shrub
Callisthene sp.	Vochysiaceae	forest, savanna, dry forest	tree
Calophyllum sp.	Clusiaceae	forest	tree
Caperonia sp.	Euphorbiaceae	aquatic	herb
Caryocar brasiliense	Caryocaraceae	savanna, dry forest	tree
Casearia sp.	Flacourtiaceae	grassland, savanna, forest, dry forest	tree, shrub
Cecropia sp.	Cecropiaceae	forest, savanna	tree

Cedrela-Type	Meliaceae	forest	tree
Celtis sp.	Ulmaceae	forest	tree
Centrosema sp.	Fabaceae	savanna, grassland, forest	bindweed, subshrub
Cestrum sp.	Solanaceae	forest, savanna, dry forest, grassland	shrub, subshrub
Chrysophyllum sp.	Sapotaceae	savanna, forest	tree
Cissampelos sp.	Menispermaceae	forest, grassland, savanna	bindweed, herb, subshrub
Cissus sp.	Vitaceae	forest, savanna	bindweed
Commiphora leptophloeos	Burseraceae	forest	tree
Copaifera sp.	Fabaceae	savanna, forest, dry forest	tree, shrub
Cordia sp.	Boraginaceae	savanna, grassland, forest, dry forest	tree, shrub, subshrub
Crotalaria-Type	Fabaceae	forest, savanna, grassland, swamp	shrub, subshrub, herb
Croton-Type	Euphorbiaceae	savanna, dry forest, grassland, forest	herb, tree, subshrub, shrub
Cuphea sp1.	Lythraceae	grassland, savanna, palm swamp, forest, dry forest, swamp	herb, subshrub
Cuphea sp2.	Lythraceae	grassland, savanna, palm swamp, forest, dry forest, swamp	herb, subshrub
Curatella americana	Dilleniaceae	savanna, dry forest	tree
Cyperaceae	Cyperaceae	forest, grassland, swamp, palm swamp, savanna, dry forest	herb
Dendropanax sp.	Araliaceae	forest	tree
Desmodium sp.	Fabaceae	savanna, grassland, dry forest, forest	subshrub, herb, shrub
Dilodendron bipinnatum	Sapindaceae	forest	tree
Diodia-Type	Rubiaceae	savanna, grassland, forest	subshrub, shrub, herb
Doliocarpus-Type	Dilleniaceae	forest, dry forest	bindweed
Drimys sp.	Winteraceae	forest, grassland	tree
Drosera sp.	Droseraceae	swamp, grassland	herb
Drymaria sp.	Caryophyllaceae	swamp	herb
Echinodorus sp.	Alismataceae	swamp, (palm swamp, savanna, forest)	herb
Eichornia sp.	Pontederidaceae	aquatic	herb
Ericaceae	Ericaceae	forest, savanna, swamp, grassland	shrub, tree, subshrub
Eriocaulaceae	Eriocaulaceae	swamp, grassland, savanna, forest, palm swamp	herb, subshrub
Eriotheca-Type	Malvaceae	forest, savanna	tree
Eryngium-Type	Apiaceae	forest, swamp, savanna, grassland	herb
Erythrina cf. speciosa	Fabaceae	savanna, forest	tree

Erythroxylum sp.1	Erythroxylaceae	forest, savanna, grassland, dry forest, swamp	tree, herb, shrub, subshrub
Erythroxylum sp.2	Erythroxylaceae	forest, savanna, grassland, dry forest, swamp	tree, herb, shrub, subshrub
Euphorbia sp.	Euphorbiaceae	savanna, swamp, grassland	herb, tree
Euplassa sp.	Proteaceae	forest, savanna	tree
Evolvulus sp.	Convolvulaceae	forest, savanna, grassland, dry forest, swamp	herb, subshrub
Ficus sp.	Moraceae	forest	tree
Forsteronia-Type	Apocynaceae	forest, dry forest	tree,bindweed
Friedericia sp.	Bignoniaceae	forest	bindweed
Galianthe sp.	Rubiaceae	grassland, swamp	herb, subshrub
Gomphrena sp.	Amaranthaceae	savanna, grassland, forest, swamp	subshrub, herb
Gomphrena sp.2	Amaranthaceae	savanna, grassland, forest, swamp	subshrub, herb
Gouania-Type	Rhamnaceae	savanna, forest	bindweed
Hedyosmum brasiliense	Chloranthaceae	forest, swamp	tree
Helicteres sp.	Malvaceae	forest, savanna, grassland	shrub, subshrub
Hyeronima sp.	Euphorbiaceae	forest	tree
Hyptis-Type	Lamiaceae	grassland, savanna, swamp, dry forest, forest, palm swamp	herb, shrub, subshrub
Ilex sp.	Aquifoliaceae	forest, savanna, grassland	tree, shrub
Iridaceae	Iridaceae	grassland, swamp, dry forest	herb
Jacaranda-Type	Bignoniaceae	savanna, forest, grassland, dry forest	tree, shrub, subshrub
Jacquemontia-Type	Convolvulaceae	savanna, forest	herb, bindweed
Lamanomia sp.	Cunoniaceae	forest	tree, shrub
Laplacea sp.	Theaceae	forest, grassland	tree
Lippia sp.	Verbenaceae	grassland, savanna, forest, swamp	shrub, herb, subshrub
Lobelia-Type	Campanulaceae	grassland, savanna, swamp, forest	herb, subshrub
Ludwigia sp.	Onagraceae	grassland, swamp, forest	herb, subshrub, shrub
Machaerium-Type	Fabaceae	forest, savanna, dry forest	tree
Maprounea-Type	Euphorbiaceae	forest, savanna, dry forest	shrub
Matayba sp.	Sapindaceae	forest, savanna, dry forest	tree, shrub,bindweed
Mauritia flexuosa	Arecaceae	palm swamp, swamp	tree
Maytenus-Type	Celastraceae	forest, savanna	tree, shrub
Melastomataceae	Melastomataceae	All	all

Melochia sp.	Malvaceae	savanna, forest, grassland	subshrub, herb, shrub
Mimosa sp.1	Fabaceae	savanna, grassland, forest, palm swamp, dry forest,	shrub, tree, herb, subshrub
Mimosa sp.2	Fabaceae	savanna, grassland, forest, palm swamp, dry forest,	shrub, tree, herb, subshrub
Myriophyllum sp.	Haloragaceae	swamp, aquatic	herb
Myrocarpus sp.	Fabaceae	forest	tree
Myroxylon sp.	Fabaceae	forest	tree
Myrsine sp.	Myrsinaceae	forest, dry forest, savanna	tree
Myrtaceae	Myrtaceae	forest, savanna, dry forest, grassland, palm swamp	tree, subshrub, shrub
Nymphaeaceae	Nymphaeaceae	aquatic	herb
Parinari sp.	Chrysobalanaceae	savanna, grassland	shrub
Peperomia sp.	Piperaceae	forest	herb
Peritassa-Type	Celastraceae	forest, savanna	shrub, bindweed
Pfaffia sp.	Amaranthaceae	savanna, grassland	herb, shrub
Phyllanthus sp.1	Phyllanthaceae	savanna, dry forest, grassland, forest	shrub, herb, subshrub
Phyllanthus sp.2	Phyllanthaceae	savanna, dry forest, grassland, forest	shrub, herb, subshrub
Piper sp.	Piperaceae	forest	shrub, tree, herb
Piptadenia sp.	Fabaceae	forest, savanna	tree
Plenckia populnea	Celastraceae	savanna, forest	tree
Poaceae	Poaceae	all	herb
Podocarpus sp.	Podocarpaceae	forest	tree
Poeppigia procera	Fabaceae	savanna	shrub
Polygala sp.	Polygalaceae	grassland, savanna, forest, swamp, palm swamp	herb, subshrub, shrub
Polygonum cf. meisnerianum	Polygonaceae	savanna, aquatic	herb
Pontederia sp.	Pontederidaceae	aquatic, swamp	herb
Pouteria sp.	Sapotaceae	savanna, forest, palm swamp	tree, shrub
Protium sp.	Burseraceae	savanna, forest, dry forest	tree, shrub
Prunus sp.	Rosaceae	forest	tree
Pseudobombax cf. longiflorum	Malvaceae	dry forest	tree
Pseudobombax cf. marginatum	Malvaceae	savanna	tree
Pterogyne nitens	Fabaceae	savanna	tree
Pyrostegia cf. venusta	Fabaceae	savanna, forest	bindweed

Rhamnus-Type	Rhamnaceae	savanna, forest	tree, shrub
Roupala sp.	Proteaceae	savanna, forest, dry forest	tree, shrub
Sagittaria sp.	Alismataceae	swamp, aquatic	herb
Sapium sp.	Euphorbiaceae	savanna, forest, grassland	tree, shrub, subshrub
Sauvagesia sp.	Ochnaceae	savanna, swamp	shrub, subshrub
Schefflera sp.	Araliaceae	forest, savanna	tree
Schinus sp.	Anacardiaceae	savanna, dry forest, forest	tree, shrub
Sclerolobium-Type	Fabaceae	savanna, forest	tree
Sebastiania sp.	Euphorbiaceae	savanna, forest, grassland	herb, subshrub, shrub, tree
Senna-Type	Fabaceae	savanna, forest	shrub, subshrub, tree, herb
Serjania sp.	Sapindaceae	forest, savanna, dry forest	bindweed
Sida-Type	Malvaceae	savanna	shrub, herb
Sloanea sp.	Elaeocarpaceae	forest	tree
Solanum sp.	Solanaceae	savanna, forest	all
Sterculia sp.	Malvaceae	forest	tree
Stryphnodendron sp.	Fabaceae	savanna, grassland	tree, shrub
Styrax sp.	Styracaceae	forest, savanna	tree, shrub
Syagrus-Type	Arecaceae	savanna, grassland, dry forest, forest	tree, shrub
Symplocos sp.1	Symplocaceae	forest, dry forest, savanna	tree
Symplocos sp.2	Symplocaceae	forest, dry forest, savanna	tree
Tabebuia-Type	Bignoniaceae	savanna, forest	tree, shrub
Tapirira sp.	Anacardiaceae	forest, savanna	tree
Toulicia-Type	Sapindaceae	savanna	shrub, subshrub
Trema micrantha	Ulmaceae	forest	tree
Typha sp.	Typhaceae	swamp, aquatic	herb
Urera-Type	Moraceae	forest	shrub
Utricularia sp.	Lentibulariaceae	grassland, swamp, aquatic	herb
Vismia sp.	Clusiaceae	forest	tree, shrub
Vochysia sp.	Vochysiaceae	forest, savanna, dry forest, grassland	tree, shrub
Weinmannia sp.	Cunoniaceae	forest	tree, shrub
Xyris sp.	Xyridaceae	grassland, swamp	herb

Zanthoxylum sp.	Rutaceae	forest, dry forest	tree

[1] from MENDONÇA, R.C.; FELFILI, J.M.; WALTER, B.M.T.; SILVA JÚNIOR, M.C.; REZENDE, A.V.; FIGUEIRA, J.S.; NOGUEIRA, P.E. 2008. Flora vascular do bioma Cerrado: um "checklist" com 11.430 espécies. In: SANO, S.M.; ALMEIDA, S.P.; RIBEIRO, J.F. (eds.), Cerrado: Ecologia e Flora. v.2. Embrapa Informação Tecnológica, Brasília, Brazil, pp. 423-1279.

[2] from Flora do Brasil 2020. Jardim Botânico do Rio de Janeiro. Available at: < http://floradobrasil.jbrj.gov.br/ >.

862

863

864

865

866

867

868

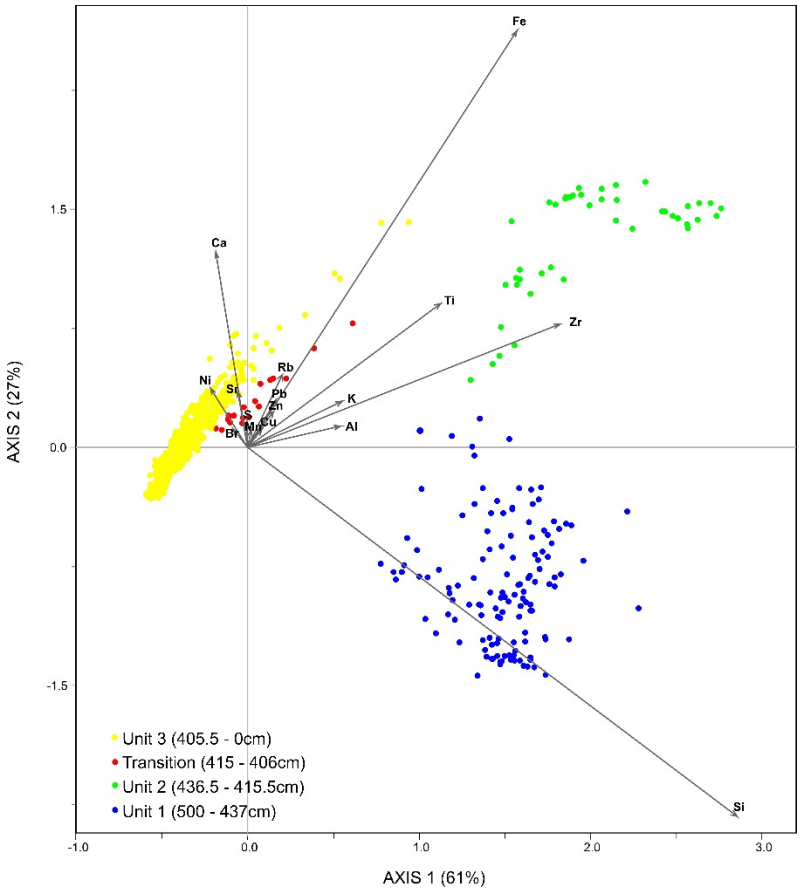
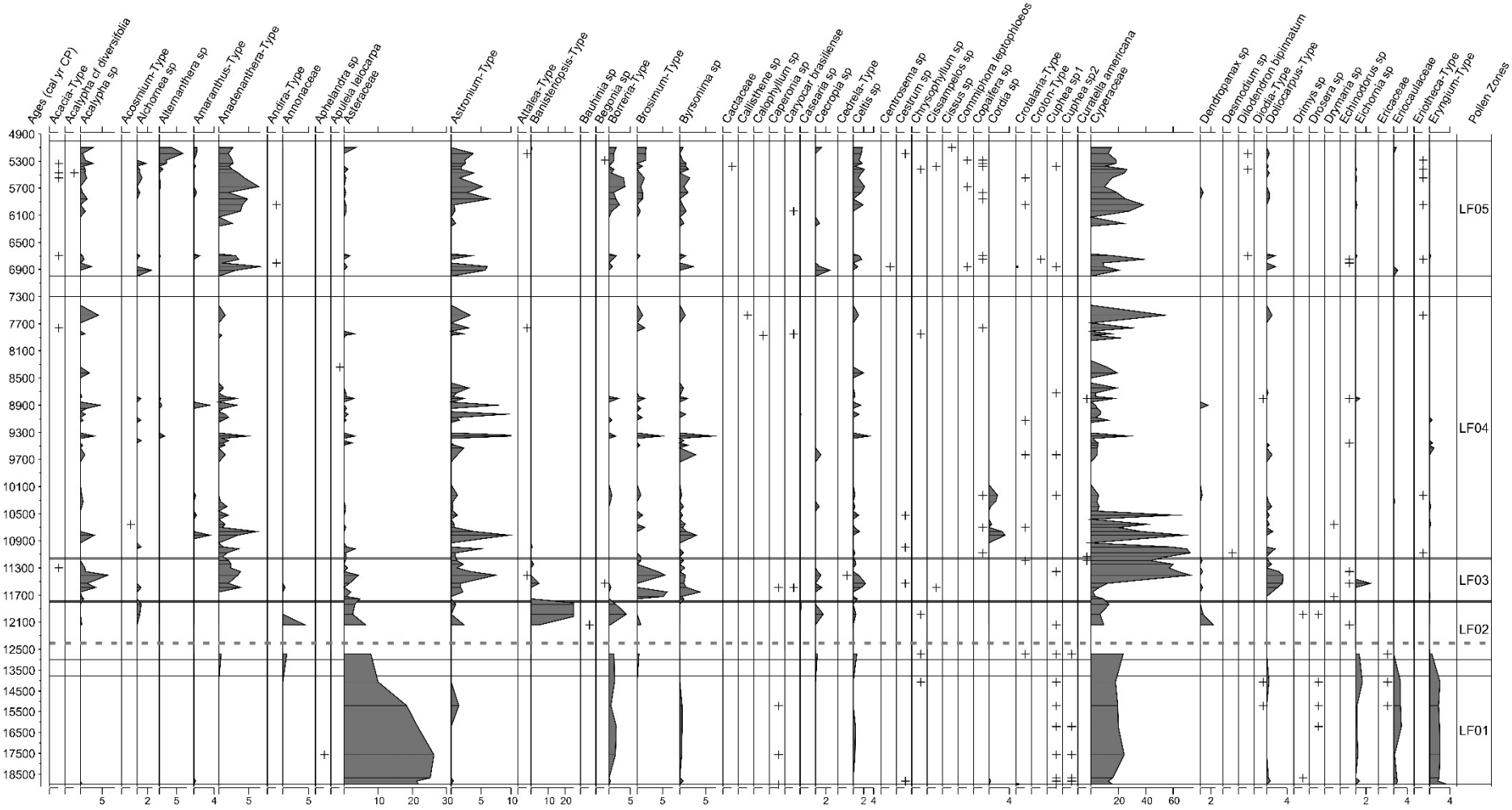


Figure 1: Principal Components Analysis biplot of the most significant elements detected through XRF scanning of the LF15-2 core. Samples from units 1, 2, and 3 are plotted in blue, green, and yellow, respectively, with the red color denoting samples at the transition phase from unit 2 to 3.

874



875

876 **Figure 2:** Complete percentage diagram for the Lagoa Feia record with all pollen and non-pollen palynomorphs (NPP). Pollen taxa are presented in alphabetic order. The
877 bottom part of the core (section below the dashed horizontal line) has a compressed age scale.

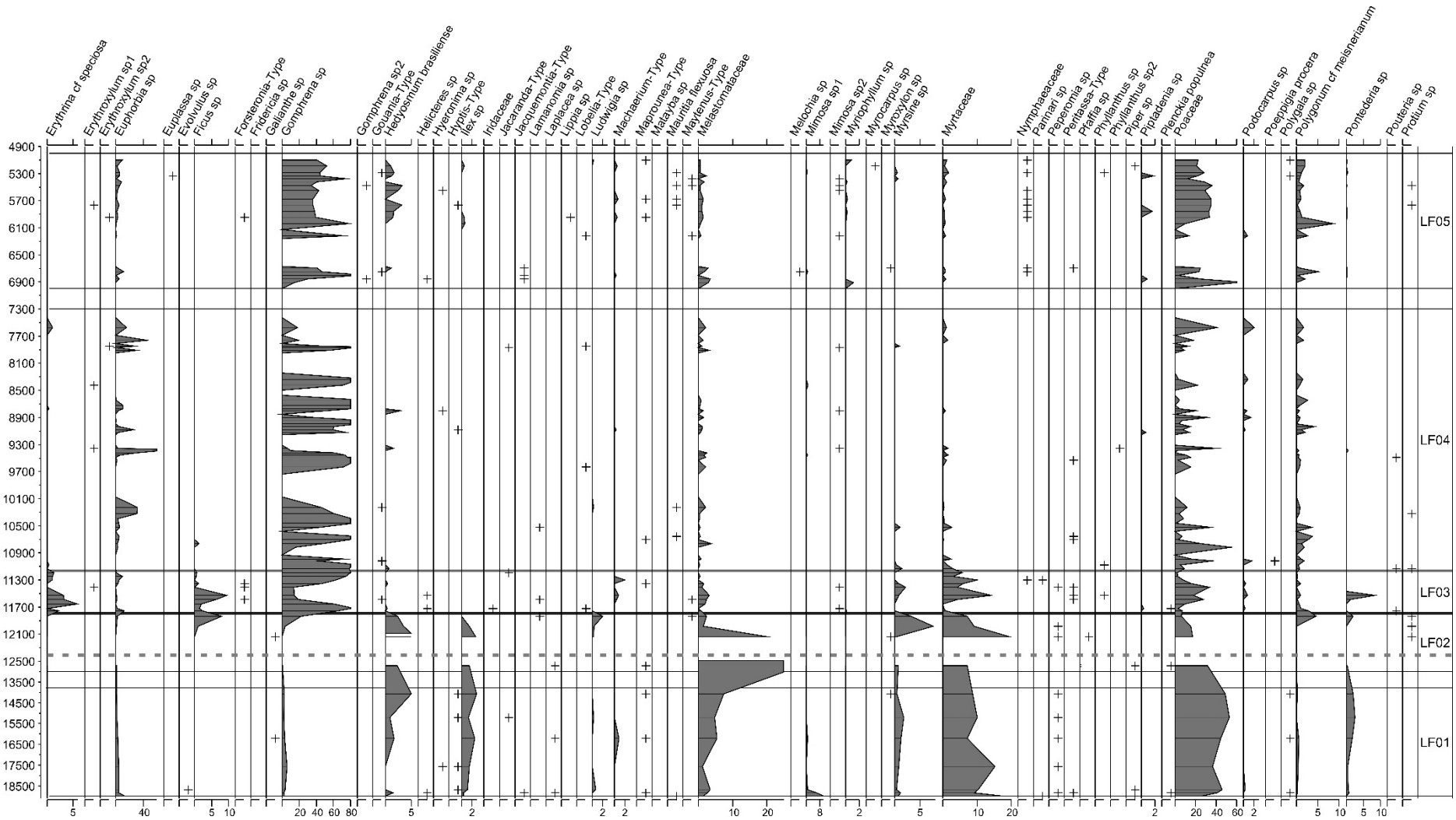


Figure 3: Complete percentage diagram for the Lagoa Feia record with all pollen and non-pollen palynomorphs (NPP). (cont.)

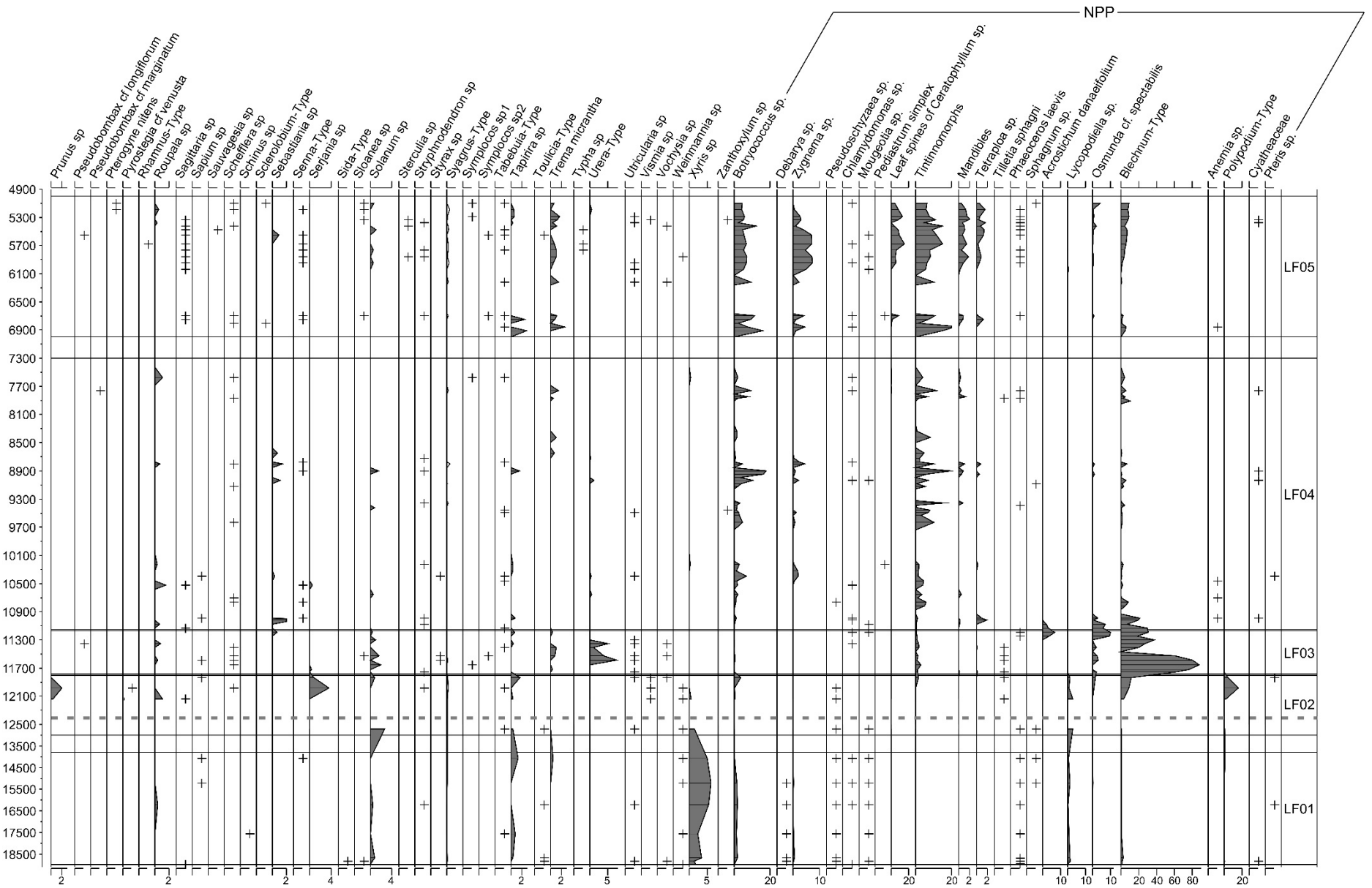


Figure 4: Complete percentage diagram for the Lagoa Feia record with all pollen and non-pollen palynomorphs (NPP). (cont.)

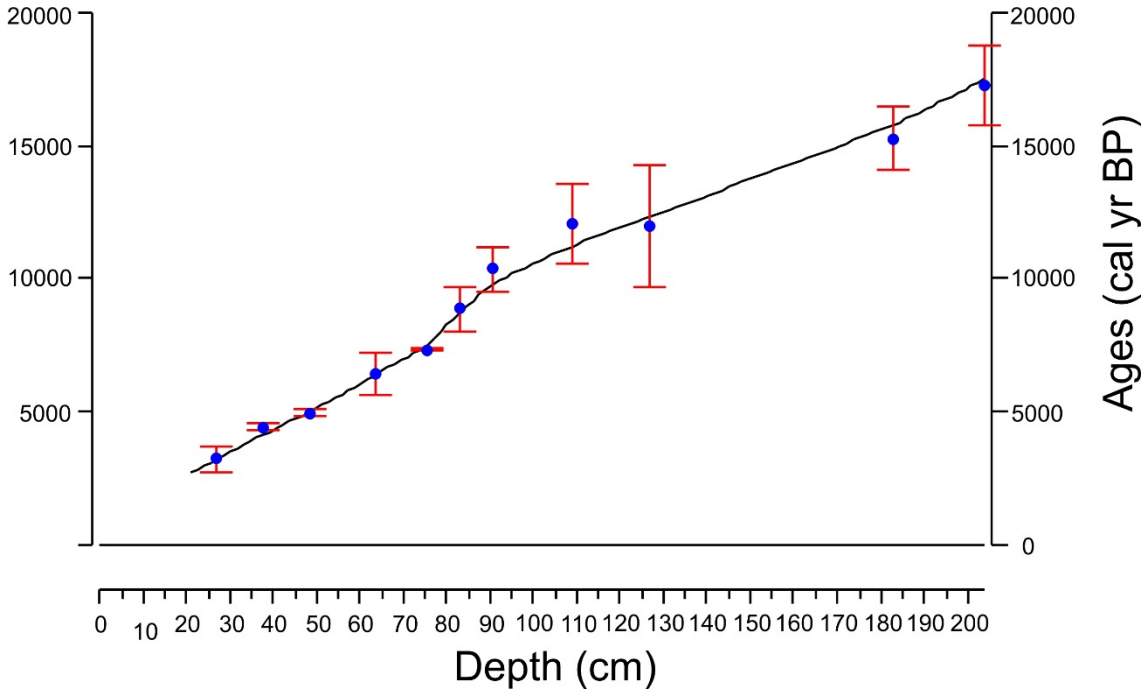


Figure 5: Age-depth model for the Salitre record (Ledru, 1993; Ledru *et al*., 1996). The Salitre record consists of a 6m core collected from a peat bog located on the top of a circular elevated area (1100 m) associated to a carbonatite plug, situated in western Minas Gerais State, Southeastern Brazil (19°S, 46°46'W). The core dates back to more than 50,000 yr BP, but the presented age-depth model only considered the upper part of the core, spanning the period between ~2,700 and 16,000 cal yr BP. The chronology of this part of the core is based on ten radiocarbon dates and the new age-depth model was built using Bacon (Blaauw & Christen, 2011).

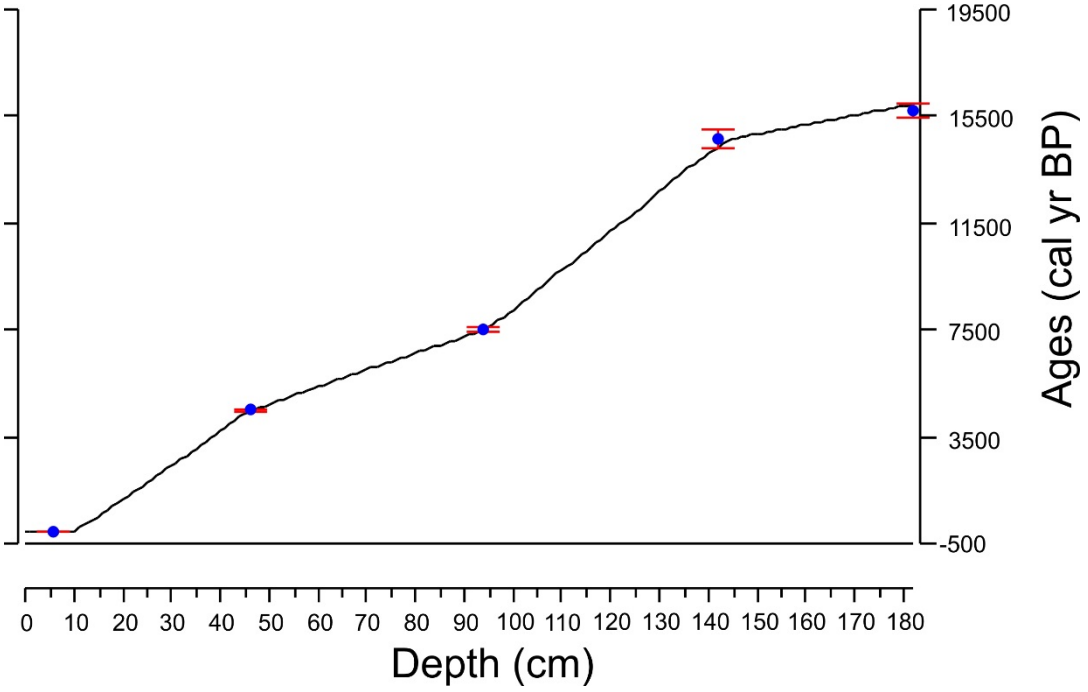


Figure 6: Age-depth model for the São José record (Cassino *et al*., 2018). The São José record consists of a 1.82 m core collected on the border zone of a *vereda* (palm swamp) located in northern Minas Gerais State (17°04'S, 45°06'W). Five radiocarbon dates were available for this core and were used to build the age-depth model with Bacon (Blaauw & Christen, 2011).